Natural Clinoptilolite Composite Coated Stainless Steel Tubular Membranes for Water Softening and Desalination

by

Solmaz Adamaref

A thesis submitted in partial fulfillment of the requirements for the degree of

Master of Science

in

Chemical Engineering

Department of Chemical and Materials Engineering

University of Alberta

Abstract

Water is an essential resource for life and sources of fresh water are limited. As population and industries are increasing around the world the need for reuse the water is increased. One of the most important industries in Alberta, Canada is oilsands industry. Steam assisted gravity drainage (SAGD) is a commercial, in-situ oil production technology in which water plays a central role. Purification of SAGD produced water is very vital for sustainable application of this technology. Researchers are motivated to develop new energy efficient methods and technologies to reuse water. Salinity is one major issue in SAGD produced water; sodium concentration in SAGD water (over 1400 ppm) is dominant as compared to other mineral ions. Therefore, to prevent scaling in boilers, desalination of SAGD water is very important for reuse of SAGD produced water. Membrane technology is the most widely used technology for water desalination.

Recently, disc membranes generated from high purity natural clinoptilolite mineral rock have shown promising water desalination and de-oiling performance. In this study a new strategy for scaling up production of these types of membranes for industrial applications was applied and developed. Natural clinoptilolite powder from St. Cloud (Winston, NM, USA) and aluminum phosphate as a binder was deposited on the inner surface of porous stainless steel tubes by dip-drain technique. Phase composition and morphology of the coating materials were investigated using X-ray diffraction and scanning electron microscopy. Besides, particle size distribution of slurry is studied. The membrane performance (permeation and

separation) in water softening were evaluated using Edmonton (Alberta, Canada) municipal tap water as feed source.

Preliminary experimental results show a high water flux of 34.20 kg/m^2.h and 91.88% and 87.03% of reduction of hardness and conductivity in a once-through membrane process at 160°C and feed pressure of 780 kPa, respectively.

These results show that natural zeolite coated stainless steel tubular membranes have great potential for large-scale desalination of industrial wastewater at high temperature and pressures. The potential application of the membrane in treatment of steam assisted gravity drainage (SAGD) produced water at high temperature and pressure will be discussed.

Acknowledgments

I would like to express my gratitude to my supervisor, Dr. S. M. Kuznicki, for his guidance, patience and support for doing this research project.

I gratefully thank W. An and Dr. J. Sawada for their valuable supports, advices, encouragements, and comments during my research.

I would like to appreciate the help of all technicians and staff in Dr. Kuznicki's group for giving me support inside and outside the lab.

I also would like to thank my family for their unconditional supports and love through my life and their encouragements during my studies.

I thank Helmholtz Alberta Initiative (HAI) for funding of this project.

Contents

List of figures

List of tables

Nomenclature

A	Membrane effective area
ALP	Aluminum phosphate
C	Concentration
C_b	Bulk feed concentration
C_f	Feed water concentration
C_m	Solute concentration near the membrane surface
C_p	Solute concentration
D	Diffusion coefficient
DDR	International zeolite association framework type code
d_h	Hydraulic diameter
DI water	Deionized water
HEU	International zeolite association framework type code
ICP	Inductively coupled plasma
IZA	International zeolite association
J_s	Mass flux
J_w	Water flux
K	Mass transfer coefficient
L	Length
LTA	International zeolite association framework type code
MFI:	International zeolite association framework type code
$\dot{m}_s$	Mass flow rate passing through the membrane
OTSG	Once through steam generator
P	Pressure
PCH	Permeate's Ca hardness
W	Weight of the permeate sample
ppm	Part per million
PSD	Particle size distribution
PTH	Permeate total hardness of the permeate water
Q_p	Volumetric flow rate that permeates through the membrane

R_{app}	Apparent rejection
Re	Reynold number
R_{int}	Membrane rejection
R_{sys}	System rejection
SAGD	Steam assisted gravity drainage
Sc	Schmidt number
SEM	Scanning electron microscopy
Sh	Sherwood number
SOR	Steam to oil ratio
T	Temperature
TCH	Tank's water Ca hardness
t	Sample collection time
TTH	Tank water's total hardness
VOCs	volatile organic compounds
WLS	Warm lime softening
WAC	Weak acid cation
XRD	X-Ray diffraction
N/A	Not applicable
2θ	Scattering angle
δ	Boundary layer thickness
u	Flow velocity
υ	Kinematic viscosity

1. Introduction

1.1. Overview

In the oil sands industry, several steps are required to make sure that the recycled water meets the boiler feed water quality requirements. These steps have been changed over time to become more cost effective and energy efficient for the sustainable in situ oil sands production by SAGD technology.

In the process of produced water[1] treatment, polymeric or ceramic membranes have been employed for several years. Polymeric membranes although show promising separation characteristics but their applications in high chemical content and operation temperature of SAGD produced water is a great chemical and thermal stability challenge for the membranes' materials. On the other hand, porous ceramic membranes are thermo-chemically stable but their separation mechanism is not applicable for water softening and desalination purposes. Synthetic zeolites on porous supports, currently, are the most popular zeolite membranes. But these zeolite membranes are expensive and lack the robustness required for industrial applications.

In a recent study, membranes of high-density, low cost natural zeolite deposits are shown a promising gas and liquid separation [1]. Scaling-up the natural clinoptilolite membranes directly sectioned from mineral deposits remained a challenge although the effective removal of both cations and hydrocarbons from SAGD water were achieved in the laboratory.

[1] Produced water is the contaminated water from by-products of oil and gas industries.

In this study, low-cost commercial natural clinoptilolite powder has been used to prepare zeolite coated stainless steel tubular membranes for water treatment. These membranes are thermally stable in SAGD water operation temperatures which are around 160°C and the energy required for extra cooling and reheating of purified feed water can be saved.

1.2. Zeolites

Zeolites were discovered in 1756 by A. F. Cronstedt, a Swedish mineralogist and since then 195 unique structures have been identified [2]. The name of zeolite is from a Greek word meaning "boiling stone" [3]. Zeolites are crystalline allumino-silicate materials with three dimensional porous framework structure and very high internal surface area. Some zeolites are minerals which are extensively mined around the world and some are synthesized for specific uses. Generally the structure of zeolites contains silicon, aluminum, and oxygen and their pores can contain water, cations or other molecules [4]. Zeolite pores are result from the self-assembly of TO_4 tetrahedra, where T is either silicon or aluminum (Figure 1). Different arrangements of TO_4 structure in zeolite makes different pore sizes and whole zeolite structure with variety properties. Features of zeolites are changeable by changing the Al-Si ratio in the zeolite structure.

Unique properties of porous zeolites make them useful for variety of applications and demand market of several million tons per annum. Natural and synthetic zeolites applications in industry can be categorized to four main groups: ion exchanging, adsorption, molecular sieving, and catalytic applications [4].

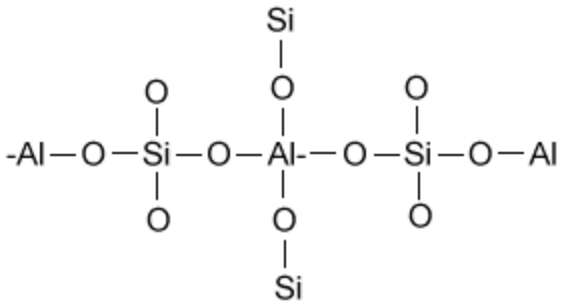

Figure 1. Basic structure of zeolite[5]

1.2.1. Natural zeolites

Natural zeolites are volcanic minerals, formed as lava rocks ash were deposited in an alkaline environment and crystallized over millions of years. Some of these unique structure mineral zeolites, due to high crystalline formation, are used for jewelry for over 200 years [6], [7]. Their unique characterizations make them valuable for industrial applications, environmental pollution control, separation science and technology. The arrangement of elements in the structure of zeolites changes the size of pores from approximately 3 to 12 angstroms depending on the type of zeolite mineral [8]. Molecular sieve is another term for zeolite, describes their ability of separating molecules by size. There are more than 40 natural zeolites that have been identified in the past two centuries, but only mordenite, clinoptilolite, chabazite, erionite, ferrierite, phillipsite, and analcime occur in sufficient quantity and purity to be exploited commercially [3], [4], [9].

Applications of natural zeolites include their use as construction material [10], filler in paper [11], use for removal of heavy metals from drinking water [12]–[16], removal of Cs and Sr from nuclear waste [17], removal of ammonia from

municipal, industrial, and agricultural waste [18], as animal feed additives [19], [20], in pet litters [20], and ammonia filters in kidney-dialysis units [21].

1.2.1. Clinoptilolite

Clinoptilolite is one of the natural zeolites from heulandite family [3], [22], [23],[24]. Heulandite (HEU) was named in 1822 by an English mineralogical collector H.Heuland [25]. Clinoptilolite was discovered by Schaller (1923)[26] and its structure was first studied by Koyama and Takeuchi (1977) and Galli at al. (1983)[27][28]. The name clinoptilolite was given due to its distinctive inclined edges and similarity to mordenite (ptilolite) [26]. Clinoptilolite and heulandite are the most abundant natural zeolites [6] and are mainly found in specific types of sedimentary rocks (tuffs). These HEU-type tuffs provide low-cost industrial minerals with several commercial applications [4].

The typical formula of clinoptilolite is $(Na^{+},K^{+})_6[Al_6Si_{30}O_{72}]\cdot 20H_2O$ and heulandite is $(Na^{+},K^{+})_1(Ca^{2+})_4[Al_9Si_{27}O_{72}]\cdot 24H_2O$ [25]. Mineralogists use several ways to differentiate between these two types of zeolites. Using cationic contents when $(Ca^{3+}Sr^{3+}B^{2+})>(Na^{+}K^{+})$ declaring heulandite while else is clinoptilolite [25], [29]. However this method is not effective when clinoptilolite and heulandite can be transformed to each other by a simple ion exchange procedure. International zeolite association (IZA) chose to differentiate heulandite and clinoptilolite based on their Si/Al ratio alone. IZA declared minerals with Si/Al greater than 4 are clinoptilolite and those less than 4 are heulandite [30]. Zeolites with higher silica

contents can stand at higher temperatures before their frameworks collapses [8], [31].

Clinoptilolite framework structure contains three sets of intersecting channels of 8 and 10 member rings. Clinoptilolite consists of a two dimensional system of three types of channels, with sizes of channel A: c-axis, 10 membered rings (4.4×7.2Å) channel B: c-axis, 8 membered rings (4.7×4.1Å), channel C: a-axis, 8 membered rings (5.5×4.0Å) [32]. Heulandite and clinoptilolite both exhibit the HEU framework. Figure 2 shows three sets of channels of HEU framework.

Pore diameter of 3-5Å make clinoptilolite an ideal candidate as a membrane material, including purification of water, which has an effective diameter of 2.6Å [6]. The dimensions of the channels of clinoptilolite framework are smaller than most hydrated cations typically present in water. This characteristic confers the potential of natural clinoptilolite for water softening and desalination applications [33], [34]. The size of hydrated ions are presented in table 1.

Table 1. Ionic and hydrated ion size

Ions	**Ionic radius (Å)**	**Hydrated radius (Å)**
Na^+	0.95[35], 1.011[36], 1.17[37]	3.58[35], 3.58[37], 2.99[38]
K^+	1.33[35], 1.377[36], 1.49[37]	3.31[35], 3.31[37], 2.75[36]
Ca^{2+}	0.99[35], 1.005[36], 1.23[39], 1[37]	4.2[35], 2.60[39], 4.12[37]
Mg^{2+}	0.65[35], 0.72[36], [37], [39]	4.4[35], 3.0[39], 4.28[37]

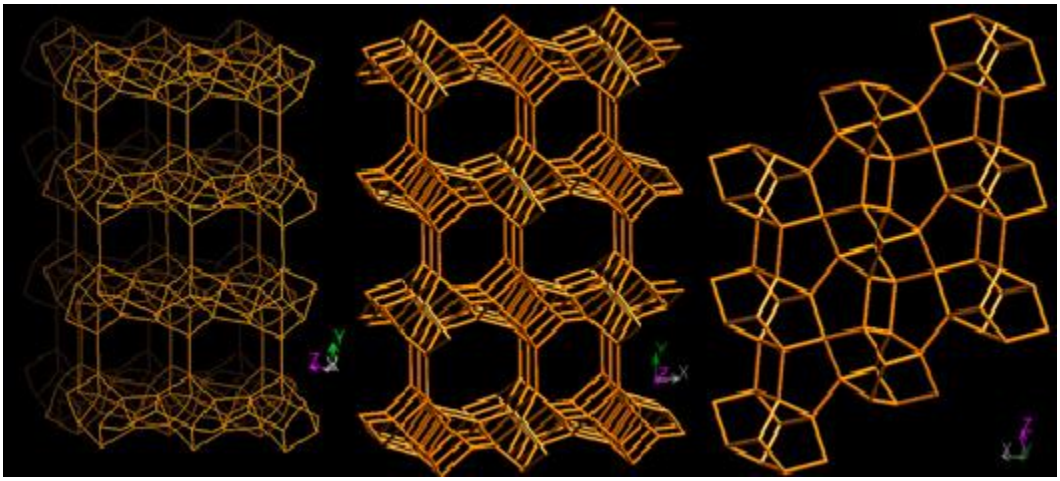

Figure 2. Unit cell structure of HEU framework: (100), (001), and (010) from left to right [30]. (International Zeolite Association Database at the website: http://www.iza-sc.ethz.ch/IZA-SC/Atlas).

1.2.2. Synthetic zeolites

The first synthetic zeolite, "zeolite A", was reported by Milton in 1948 [6]. Synthetic zeolites crystal sizes are smaller than their natural analog, and their purity and uniformity made them unique as catalysts and adsorbents [6], [7]. Over 40 years more than 150 different synthetic zeolites are commercialized such as: zeolite X, zeolite L, zeolite P, ZSM-5, silicalite, mordenite, zeolite A, zeolite Y, zeolite beta, and MCM-48 [4], [40], [41].

1.3. Membrane and membrane separations

The membrane separation process is based on the presence of a semipermeable membrane which allows one component to transport through, while others to be retained. The component that passes through the membrane pore size is permeate and everything else is retained on the feed side is retentate. This phenomena was first discovered by accident in 1748 by Nollet [42]. After Gibb's developed the

concept of free energy in 1873, the mystery of what Nollet was found was released. Since then lots of researchers devoted their time to work in membrane transport mechanism and develop the application of membranes [42].

The selectivity and productivity are factors that determine membrane performance. Separation factor or selectivity expresses the ratio of permeation of specific species to its retention and flux expresses the productivity of membrane [43].

Membrane materials can be classified to three groups: biological, organic, and inorganic [44]. Polymeric membranes as an example of organic membranes are not thermally, chemically, and mechanically stabel in harsh[2] conditions, although they are used extensivily in industry. On the other hand, inorganic membranes can withstand high thermal, chemical, and mechanical conditions [45], [46].

1.3.1. Inorganic membranes

Inorganic membranes are good candidates for a separation processes. Their applications are in high temperature, high pressure gas separation, aggressive liquids treatment, and high temperature membrane reactors. Inorganic membranes, such as zeolite, carbon, alumina, and silica membranes are generally used for separation processes due to their thermochemical stability under harsh conditions, incompressible pore structure, and the possibility of achieving very high fluxes and selectivity in specific processes [47].

[2] High thermal, chemical and mechanical conditions.

Membranes with very high selectivity are save energy because the transport of species from the feed to the permeate side at the same chemical potential occurs without energy dissipation. For achieving high selectivity, membrane microstructure and chemical composition are considered as important factors [47].

Ceramics such as: alumina (β-Al_2O_3, α-Al_2O_3), zirconia (ZrO_2), titania (TiO_2), ceria (CeO_2), glass (SiO_2), and metal sintered steel fibers or powders or thin- or thick-film deposits on various support media are mostly used for manufacturing inorganic membranes [45]. Ceramic membranes have outstanding stability at high temperatures and extreme pH [47], but their separation mechanism is not applicable for water softening and desalination [48], [49].

Zeolite membranes are unique in gas and liquid separation industries where they show some unique advantages in selectivity, flux, thermal, or chemical stability. The permeate flux of LTA type zeolite membranes is about 100 times higher than polyacrylonitrile membrane at the same H_2O/alcohol selectivity. NaA membrane which is a LTA type zeolite has a strong hydrophilic nature which makes it excellent in water separation applications however its separation mechanism is not molecular sieving. In addition, NaA zeolites are not able to work in acidic media. Another type of zeolite membrane which is considered for industrial applications is MFI type membranes [50], [51]. Other type of zeolite membranes such as silicalite, ZSM-5, mordenite, zeolite A, zeolite Y, zeolite beta, and MCM-48 [4], [47], [52] each has a unique application as zeolite membrane, but still more work and study are needed for large-scale applications [51] as manufacturing defect free membranes for commercial scales is still a challenge for synthesized zeolite

membranes. Therefore, there are few separation processes which are using synthesized zeolites such as alcohol dehydration [53] and some high-resolution molecular separations [54].

On the other hand, there are lots of low cost natural zeolites with very small pore sizes and ability to prevent ion migration through their structure in the environment. Natural zeolites are valuable due to their ability to be used in high temperature, pressure, and chemical separation processes. This kind of membranes are demanded mostly where feed streams are at high temperatures, no need for extra cooling [51] is required.

1.3.2. Zeolite membranes permeation mechanisms

Mechanism of molecules' transportation from feed side to the permeate side through the zeolite membrane are similar for both gas and liquid processes [44], [47], [51], [55]. This is because of same transport mechanism in the molecular scale for both gas and liquid systems. There are many parameters that control the transport mechanism in separation process such as temperature, pressure, molecular weight, kinetic molecular diameter, pore diameter, molecular collision-free path, heat of gas adsorption and thermal activation energies [51].

Permeation through zeolite pores occurs generally in three steps: diffusion through bulk phase to the membrane surface, mass transfer from the film adjacent to the membrane surface onto the porous material and then diffusion through the porous material. Same steps are happening in the permeate side [56]. Diffusion process through membrane depends on many factors such as: the phase of the system, the

pore size, the size of the permeating molecules and the driving force [57]. In membranes' separation process several mechanism and transport of molecules can be occurring. In figure 3 four mechanisms for molecular flow in membrane media are shown: Bulk flow, molecular diffusion, molecular sieving, and solution-diffusion.

From figure 3A it is shown that bulk flow mechanism is happening through macroporous defects with pore sizes larger than molecular diameter. In this mechanism, a mixture of different sizes of ions and other materials in the water can easily pass through the membrane without any selective separation. Molecular diffusion is shown in figure 3B occurs when pressure is equal on both sides of the membrane and transport is due to a gradient in fugacity, activity, chemical potential, concentration or partial pressure [56]. Separation mechanism of microporous membranes having pore sizes so small that they just allow specific molecules to pass through the membrane structure is shown in figure 3C. For zeolite membranes this size exclusion separation is called molecular sieving, which is an ideal separation mechanism [58]. For dense membranes solution- diffusion mechanism is proposed. This transport mechanism is based on dissolving the molecules into membrane and transport across the membrane to the permeate side [59].

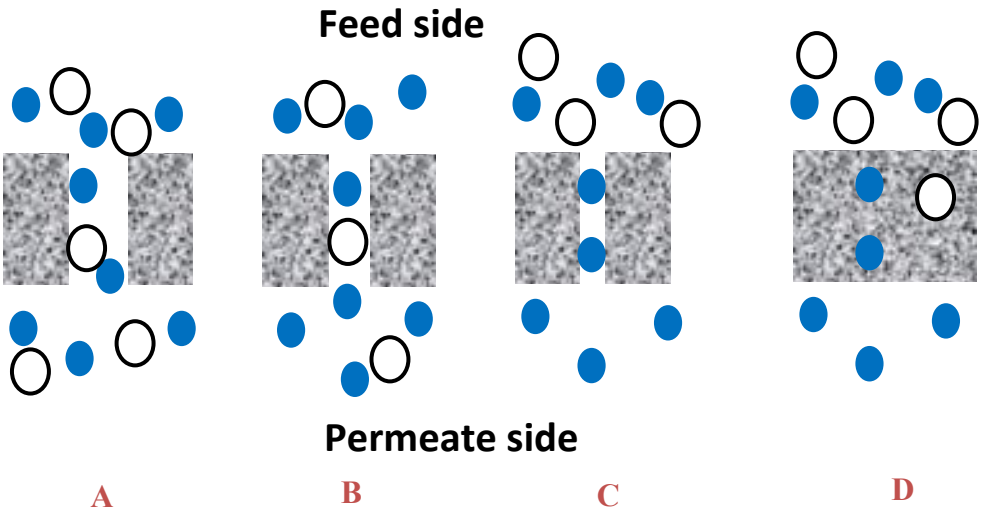

Figure 3. Transport mechanism through membrane media A) bulk flow B) molecular diffusion (Knudsen diffusion) C) molecular sieving D) Solution-diffusion.

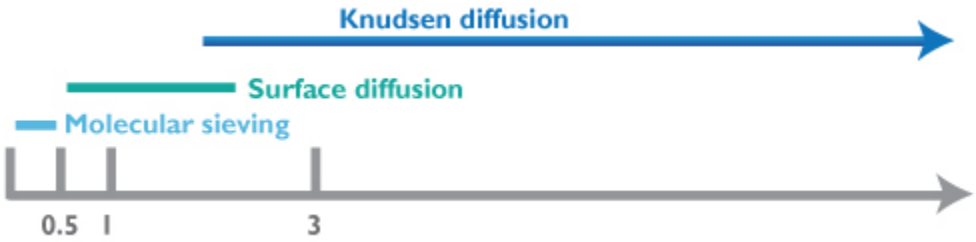

Figure 4. Correlation of membrane's pore size (in nanometer) with transport mechanism [60]

For natural zeolites due to the large range of pore sizes in their structures, first three transport mechanisms, which are mentioned above, are occurring. In a high grade natural zeolites there is less bulk flow (macroporous) and more molecular sieving transport.

The above discussion about adsorption and diffusion represent the ideal case that permeation occurs only through zeolite pores. However, in a synthesised zeolite membranes and even in composite-zeolite membranes non-zeolite pores exists. Molecules transport in non-zeolite pores have different adsorption and diffusion properties than those in zeolite pores. Therefore, Non-zeolite pores affect flux and selectivity during the separation process.

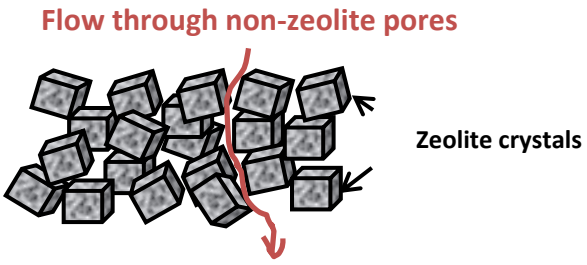

Figure 5. Flow through non-zeolite pores [58].

1.3.2.1. Parameters for evaluation of membrane performance

Membrane performance in a liquid system is determined by two key parameters, water flux and rejection (selectivity). The water flux is refers to the amount of water passing through a unit of membrane area in a specific time duration. Water flux J_W is defined as:

$$J_W = {Q_p}/{A} \quad (\text{m.s}^{-1}) \qquad (1)$$

Q_p : Volumetric flow rate that permeates through the membrane ($\text{m}^3.\text{s}^{-1}$)

A: Membrane area (m^2)

Similar to the water flux, mass flux of a solute can be defined as:

$$J_s = {\dot{m}_s}/{A_m} \quad (\text{kg.s}^{-1}.\text{m}^{-2}) \tag{2}$$

$\dot{m}_s$: Mass flow rate passing through the membrane (kg.s^{-1})

A_m : Membrane area (m^2)

The membrane rejection is defined as retention ability $R_{int}$where C_p is the solute concentration in permeate side and C_m is the solute concentration near the membrane surface [61].

$$R_{int} = 1 - \frac{C_p}{C_m} \tag{3}$$

Where C_p can be determined from below equation:

$$C_p = {J_s}/{J_w} \tag{4}$$

J_s: Solute mass flux

J_w: Volumetric water flux

As C_m in equation 3 is not known as a priori, therefore C_b is replaced in the equation as a bulk feed concentration and membrane rejection defines as apparent rejection (R_{app}) [61]:

$$R_{app} = 1 - \frac{C_p}{C_b} \tag{5}$$

The main reason that make equation 3 and 5 unequal is concentration polarization. Due to the concentration polarization $C_m \geq C_b$, Thus $R_{int} \geq R_{app}$ [62].

1.3.2.2. Concentration polarization:

Concentration polarization is a phenomenon that occurs near the surface of pressure-driven membranes. The concentration polarization occurs when non-permeable molecules (solute) in the feed flow accumulates at the membrane surface, and its concentration near the membrane surface is increased to higher levels than in the bulk [44], [56], [63]. This phenomenon has a profound effect on permeation and selectivity of the membrane. This phenomenon may occur even when the separation of solute from solvent is not perfect. Factors that can cause concentration polarization are low viscosity, low flow rate, low concentration of the permeate molecule, fouling, and membrane module design [62]. For reducing the effect of concentration polarization in zeolite membranes on supports, zeolite layer should be coated on the feed side [58], [64]. Therefore in this study, clinoptilolite composite layer is coated inside the stainless steel supported tubes.

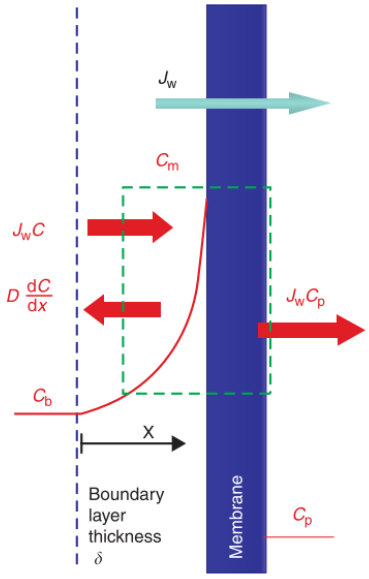

Figure 6. Concentration polarization over a membrane surface [62].

Figure 6 shows the mass balance near the membrane surface. Mass balance of the solute in the control volume is:

$$J_W C - J_W C_p - D\frac{dC}{dx} = 0 \quad (7)$$

Boundary conditions:

$$C = C_b \qquad at \qquad x = 0 \quad (8)$$

$$C = C_m \qquad at \qquad x = \delta \quad (9)$$

From solving above equations:

$$\frac{C_m - C_p}{C_b - C_p} = \exp(J_w/K) \quad (10)$$

K: mass transfer coefficient

In a special case when C_p is negligible equation 10 becomes:

$$\frac{C_m}{C_b} = \exp(J_w/K) \quad (11)$$

Equation 10 shows that at higher water flux and lower mass transfer coefficient concentration of solute in permeate, C_p increase. Therefore, membrane surface concentration C_m can be higher than bulk concentration C_b at high flux and/or low mass transfer coefficient. Mass transfer coefficient depends on Sherwood number Sh, which related to Reynolds number Re, and Schmidt Sc, and it can be summarized in equation 12:

$$K = a.D^{2/3}u^b\vartheta^{\frac{1}{3}-b}d_h^{b+d-1}L^{-d} \quad (12)$$

Where d_h is the hydraulic diameter, u the flow velocity, and υ the kinematic viscosity.

From this equation we can find out that as molecules size become bigger, lower diffusion coefficient ($D^{2/3}$) occurs and it is more likely to have concentration polarization near the membrane surface. In addition, at larger flow velocity in a cross-flow module the mass transfer coefficient increased [61], [65], [66]. In cross-flow modules there is more chance for non-permeating molecules to be carried away instead of concentrating at the membrane surface [62].

1.3.3. Zeolite membrane on support

Suzuki first reported zeolite membranes on porous metal, Vycor glass, or ceramic supports in 1987 by "in-situ direct crystallization" method [67]. After that two other methods have been developed for synthesizing zeolites on porous supports: dry and wet gel conversion method and seeding and secondary growth [51], [68]. These new zeolite membranes were synthesized either stand-alone or on tubular- or disc-shaped supports. Due to poor mechanical strength of unsupported zeolite membranes [69], in most recent work zeolite membranes are prepared on or within porous supports. Most of inorganic materials used for membrane applications are synthesized zeolites on porous supports with several layers [70]. The resistance of the membrane structure is increased by making a thin membrane layer on the smooth and strong support structure. However, by decreasing the membrane's thickness, selectivity would be decreased as a result of defects in the membrane [47]. In general, zeolite membranes with smaller thickness, less intercrystalline

gaps, and oriented structure are preferred [41], [45], [70], [71]. Most of synthesized zeolites on porous supports have polycrystalline structure and thickness between 5-30 μm. There are also several studies on zeolite membranes with thickness less than 1μm [45]. α-alumina and stainless steel are the most commonly used supports for zeolite membranes [45].

For choosing the best support to grow zeolite crystals on supports, compatible chemical and physical characteristics between the support material and the first layer of synthesized zeolite are required. When these materials are not compatible, the zeolite layer is more likely to detach, crack, or defect in a different circumstances which zeolite crystals and support material have a different behavior, such as high temperature, or pressure conditions [45]. There are different methods or techniques for growing zeolite crystals on the support, but most of the time a post treatment is also required to fill the voids and gaps in the thin film. However, the process of post treatment is time consuming, tedious and difficult as a single fracture can make the membrane ineffective.

In this study natural zeolite clinoptilolite powders from St. Cloud's deposits are applied on the surface of stainless steel tubular support to separate ions from water. This natural zeolites with unique zeolitic structure in the form of rocks (Figure 7) showed a good performance for gas and water separation [1], [33]. Despite being thermally stable and high rejection and water flux, geomorphic zeolite membranes are limited by the size of the rock sections. The powder form of clinoptilolite was a good candidate to be replaced with rock sections. In this study the natural zeolite

powders are coated inside the stainless steel tubular support for different membrane applications.

Figure 7. Natural zeolites rock section that is used for liquid separation [1].

1.4. Zeolite membranes for oil sands produced water treatment

Water is the essential source of life and it is currently estimated that by 2025 the volume of water used by industry will increase above 50% than levels in 1995 [72]. As the access to fresh water becomes limited in the world the need to reuse the process water or the need for desalinated seawater will be increased.

Oilsands is one of the main energy resources in Canada and its extraction is essential for the economy of the country. Steam assisted gravity drainage (SAGD) is the most common in situ bitumen and heavy crude oil production technology that were developed in late 1970's by Dr. Roger Butler with Imperial oil [73]. In SAGD technology two horizontal wells are drilled into the oil reservoir, one carry the high pressure steam in the upper wellbore and the lower wellbore carry the oil. The steam that goes through the upper wellbore reduces the oil viscosity and it causes oil to drain into the lower wellbore (Figure 8) [73]. Steam to oil ratio (SOR) that shows

the SAGD operation performance is in the range of 2-4 [74]. It means for every barrel of oil, 2-4 barrels of water are needed. Therefore, for the sustainability of the SAGD process and oilsands production in Canada, recycling maximum amount of water is vital.

The produced water from SAGD process is contaminated with soluble organics, dissolved silica and high ion concentrations which can cause significant scaling in boilers or steam generators. SAGD water treatment contains three main stages, primary, secondary, and tertiary [75]. The primary stage is bitumen/water separation unit; after this stage water goes to the de-oiling unit. The tertiary stage consists of either a chemical treatment or an evaporator unit. These stages are required to make sure that the recycled water meets the boiler feed water quality or a once through steam generator (OTSG) requirements. The chemical treatment consists of warm lime softening (WLS) for reducing the amount of silica and magnesium followed by multimedia filtration to remove suspended solids and weak acid cation (WAC) exchange for hardness (calcium) removal [76], [77]. Both systems (the evaporator and chemical treatment) have their own advantages and disadvantages. The disadvantages of chemical treatment unit are: high chemical dosing usage, solid waste problem, and maximum ~ 80% water recovery [78]. The disadvantages of evaporator unit are: the high energy consumption and drum boiler sensitivity to water quality [78]. Two diagram of this process can be seen in figures 9 and 10.

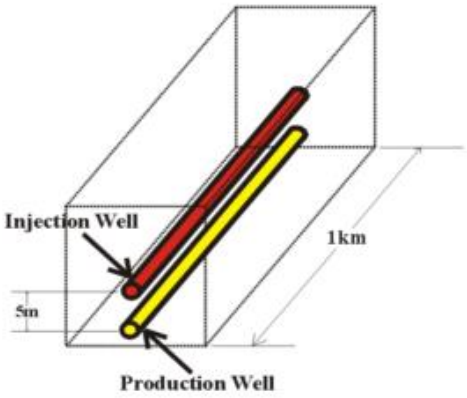

Figure 8. Schematic of two horizontal wells drilled into the oil reservoir. Steam is injected to the upper (red) well, while oil is carried up from the lower (yellow) well [73].

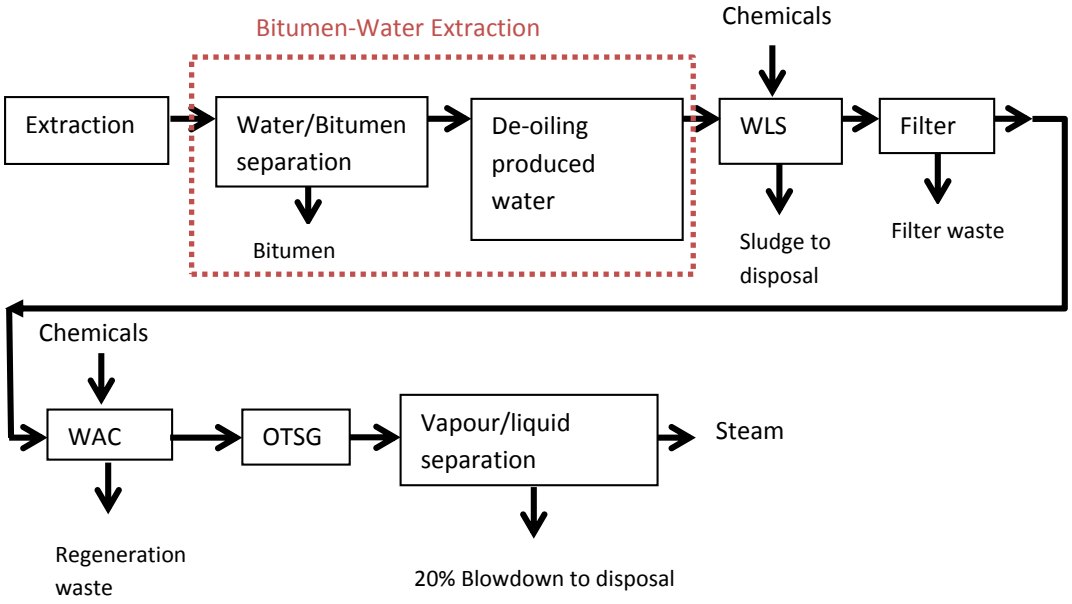

Figure 9. Chemical treatment of SAGD produced water treatment unit (Adopted from [75])

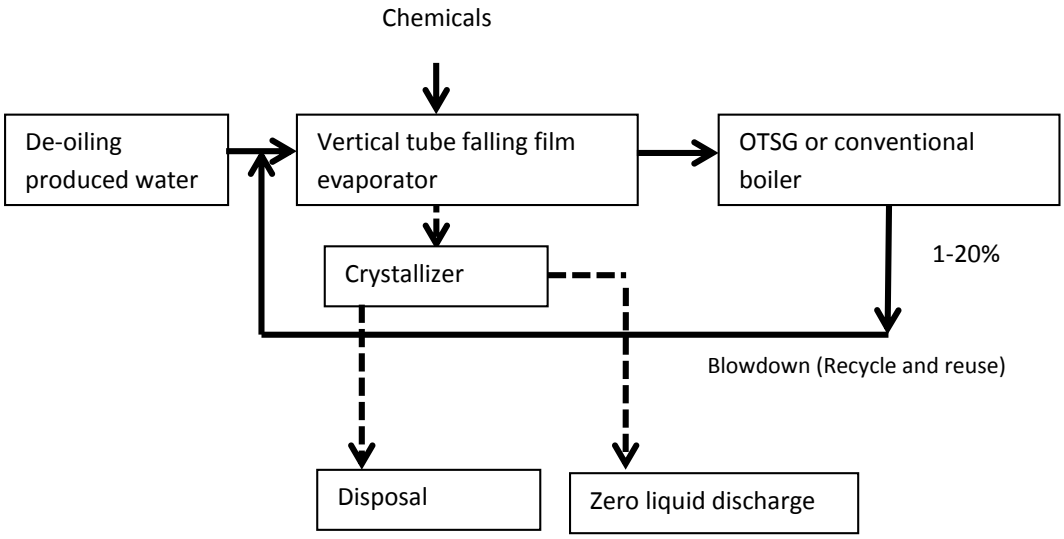

Figure 10. Evaporator unit of SAGD produced water treatment (Adopted from [75]).

2. Materials and Methods

2.1. Natural zeolite characterization

The natural zeolite clinoptilolite powder was from St. Cloud's deposit (Winston, New Mexico, USA) with particle size passed through 325 mesh sieve or below 43μm.

Table 2. Physical properties of natural zeolite clinoptilolite (Adopted from [79])

Bulk Density (In Place, dried)	87 lbs/ft^3 (1,390 kg/m^3)
Bulk Density (Aggregate, dried. Common sizes) -325 Mesh	43-47 lbs/ft^3
Clinoptilolite content	75 to 85%
Cation Exchange Capacity (CEC)	0.8 – 1.2 meq/g
Surface Charge density	10.1E-23 meq/Å^2
Color	White (85 optical reflectance)
Crushing Strength	2,500 lbs/in^3 (176 kg/m^3)
Hardness	3.5-4.0 Mohs
LA Wear (Abrasion Index)	24
Molecular Ratio	5.1 (Si/Al)
pH (natural)	7.5 to 8.0
pH Stability	0-13
Permeability	10-3 m/sec (1.4 – 0.4 mm particles)
Pore Size (diameter)	4 - 7 angstroms
Pore Volume	≤ 52%
Resistivity	~ 9,000 ohms/cm
Specific Gravity	2.2 - 2.4:1
External Surface Area	14 to 15 m^2/g
Total Surface Area	≤ 800 m^2/g
Swelling Index	Nil
Thermal Stability	1,2020 F (6500ºC)
Other	non-soluble, non-slaking, free flowing, readily mixable

2.2. Support (porous stainless-steel tube) characterization

Porous stainless steel (316L) tubes (Figure 11) provided by Graver Technologies (Glasgow, Delaware, USA) were used as zeolite composite membrane supports. The 316L stainless steel contains molybdenum which increases the resistance of steel to corrosion. These stainless steel cross-flow membranes are designed for working in harsh flow conditions, such as, high temperature, harsh chemical, high viscosity, high pressure, and high solids loading applications. Another advantage of stainless steel is its good weld-ability to metallic industrial components.

The porous stainless steel tubular substrates used in this study have a pore size range from 0.02 to 2µm. The tubular substrates with 0.02µm pore size were sintered titanium oxide pre-coated stainless steel. The thickness of TiO_2 coated layer is about 10µm.

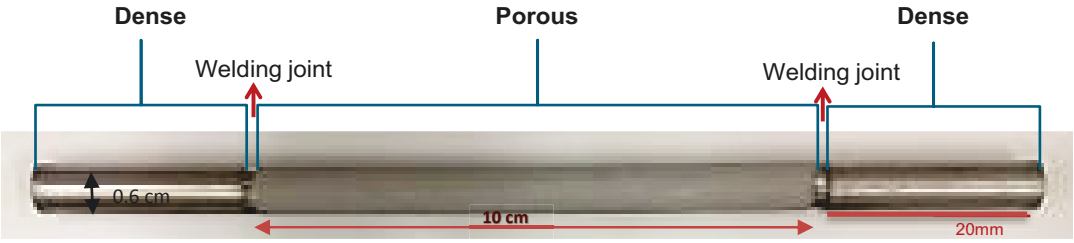

Figure 11. Stainless steel membrane support.

Figure 12. Weld-ability of porous stainless steel tubes (Adopted from[80]).

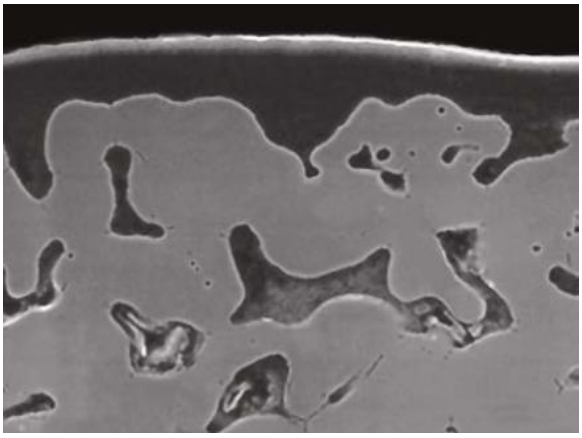

Figure 13. Cross section of titanium oxide pre-coated stainless steel tubular support. 1000× magnified (Adopted from [80]).

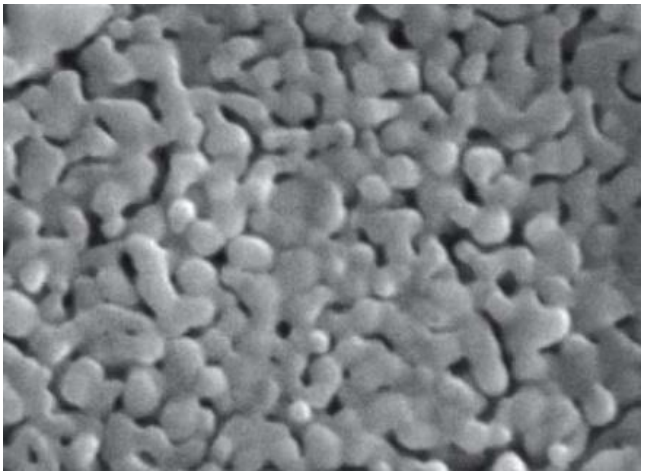

Figure 14. Sintered TiO_2 layer on stainless steel support tube. 20,000× magnified (Adopted from [80]).

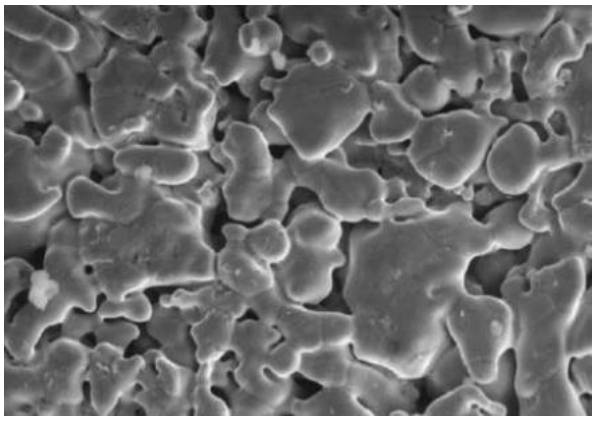

Figure 15. Sintered stainless steel membrane support. 500× magnified (Adopted from [80]).

2.3. Binder characterization

Aluminum phosphate has been widely used as a binder for ceramic coating [81],[82]. Silicate, which is the backbone structure of alumino-silicate zeolites, has similar chemical properties with phosphate which suggests the possibility of a strong chemical bonding between the phosphate and zeolite [82], making it a promising binder material for this particular applications.

Commercial aluminum phosphate based binder was purchased from Accumet Materials, (Ossining, NY, USA). This commercial type of aluminum phosphate solution can withstand temperatures up to 1650°C. This binder contains no volatile organic compounds (VOCs), is non-flammable, and is environmentally safe [83]. Table 3 shows inductively coupled plasma (ICP) results for aluminum phosphate (ALP) solution. The weight ratio of P to Al has an effect on wear-resistance of ALP_ceramic coatings [81]. The results show P/Al weight ratio in the binder solution was about four.

Table 3. Ions' concentrations in ALP solution

Analyte	***Na (ppm)***	***Mg (ppm)***	***Al (ppm)***	***P (ppm)***	***K (ppm)***	***Ca (ppm)***
Concentration in ALP solution	383	10.5	55823	226469	7.02	252

2.4. Test water quality

For the screening test of membranes municipal tap water from the City of Edmonton, Alberta Canada was used as test water to evaluate membrane performance for water softening. Tap water was chosen because the supply is not limited and the composition is relatively stable over time. The properties of Edmonton tap water is listed in table 4.

Table 4. Property of Edmonton tap water, September 2013 [84]

Parameters	**Unit**	**Monthly Average**	**YTD* Min**	**YTD* Max**
Bromate, dissolved	mg/L	<0.005	<0.005	<0.005
Chloride, dissolved	mg/L	3.78	2.40	11.00
Conductivity	µS/cm	343	301	485
Hardness, Calcium	mg $CaCO_3$/L	110	84	258
Hardness, total	mg $CaCO_3$/L	161	130	303
Nitrate (as N), dissolved	mg/L	0.01	<0.01	0.08
Nitrite (as N), dissolved	mg/L	<0.01	<0.01	<0.01
PH	N/A	7.8	7.3	8.3
Potassium	mg/L	0.83	0.60	2.82
Sodium	mg/L	7.6	3.2	25.5
Sulphate, dissolved	mg/L	47	39	131
Total organic carbon	mg/L C	1.9	1.3	3.8

*YTD:Year-to-date

2.5. Membrane preparation and characterization

2.5.1. Mixing

The stainless steel tubular substrates were washed by an alkaline detergent solution (Decon Labs, King of Prussia, PA, USA) and then rinsed thoroughly with distilled water in an ultrasonic bath for at least one hour to remove any mechanical grease during fabrication. They were then soaked in distilled water until an hour before coating deposition. Same weight ratios of clinoptilolite powder, aluminum phosphate (ALP) solution and DI water were mixed together as our coating material. The coatings were applied to the inner surface of stainless steel tubular

substrates. Two mixing procedures are used to make natural clinoptilolite-ALP composite coating slurries for the coating process.

In the first method, ALP and DI water were thoroughly mixed together for about 30 minutes to 1 hour under stirring at 350 rpm, and then clinoptilolite powders were added to the mixture and stirred at 700 rpm for about 2-3 hours.

In the second method, three ingredients of clinoptilolite powder, ALP and DI water were mixed in one step by a planetary ball mill machine (Laval Lab, Laval, QC, Canada) at 300 rpm for 20 minutes.

2.5.2. Coating

The resulting slurries were used to coat the inner surface of the porous stainless steel tubes by a dip/drain process. Dip coating method is the straight forward technique that is used in many industrial processes such as protection, magnetization, controlling refractive index, and lubrication. In this method by immersing a substrate into a reservoir of solution completely and withdrawing the substrate from the solution bath, a thin film of solution can be coated onto the substrate. The film thickness depends on many factors such as drain speed, gravitational acceleration, rate of solvent evaporation, surface tension, number of dip cycles, physical properties of the fluid, etc.[85]–[90] .

In this study, the coating slurry was injected into a vertically positioned porous stainless steel tube from the bottom using a syringe pump at a controlled flow rate (Figure 16). When the tube was completely filled with the coating slurry, the pump

was stopped and the syringe was detached from the bottom of the tube. The excess slurry was then drained out from the tubular substrates. The coated tubes were then dried at room temperature overnight and then heat treated in an electric furnace at 371°C for 4 hours. Subsequent coating layers were deposited using the same procedure. The fabricated tubular membranes (Figure 17) were soaked in distilled water until one hour before testing.

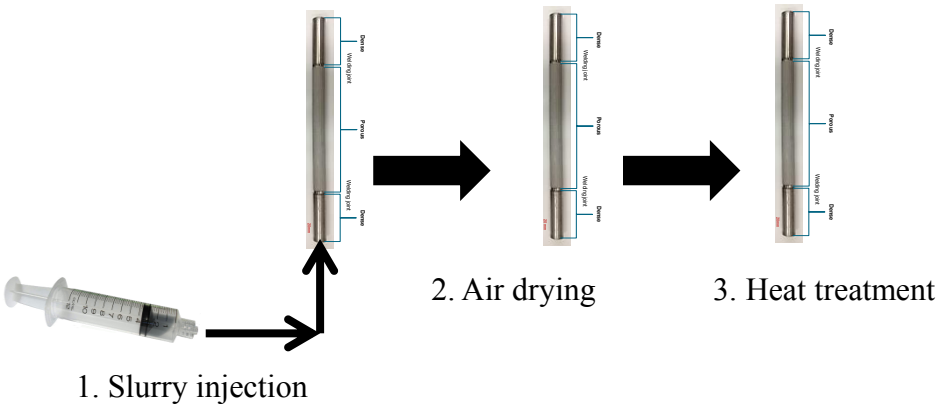

Figure 16. Schematic of the dip/drain coating procedure

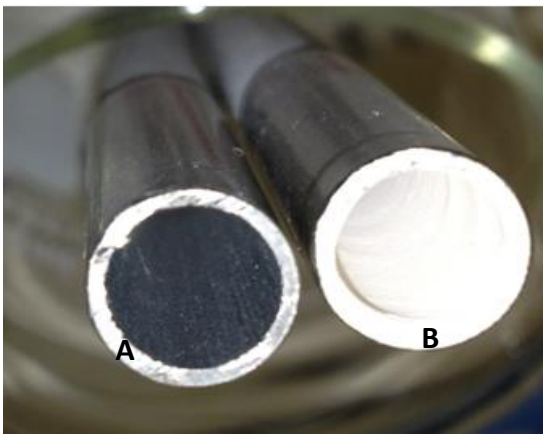

Figure 17. Stainless steel tubular supports A) before coating B) after coating

2.5.3. Characterization

To investigate the phase composition of the composite membrane material by X-ray diffraction (XRD), the coating slurry was poured into a flat plastic tray. After drying at room temperature overnight, a flat hard sheet was formed and detached from the tray and subjected to the same heat treatment as with the coated tubes. XRD patterns were collected by Rigaku Geigerflex Model 2173 diffractometer (Rigaku Corporation, Tokyo, Japan) with a Co tube and a graphite monochromator. The diffractometer was operated at 38kV and 38mA. The scan angle range was from 2θ = 1 to 90° at a step of 0.02°.

Surface morphologies of the coated tubular membranes were observed by Scanning Electron Microscopy (SEM, Hitachi S-3000N) to characterize the different morphological regions in the fabricated membranes.

Particle size distribution of clinoptilolite powders in water, mixed slurry by stirrer, and mixed slurry by ball mill machine were studied. The instrument that calculates the particle size distribution of three samples uses a dynamic light scattering technique (Mastersizer 3000, Malvern Instruments, UK). The instrument is analyzing the laser scattered diffraction pattern off of a small quantity of powder material suspended in water.

2.6. Tubular cross-flow membrane test system for water softening

Two tubular cross-flow membrane test systems were set-up for the water softening experiments at low temperature (25°C to 100°C) and high temperature (100°C to

160°C). Figure 18 shows the schematics of the low temperature setup. The pipe between heater and membrane was insulated to reduce the amount of heat loss. The tank water temperature was controlled by an immersion heater with a temperature controller. An overhead stirrer was used to mix the tank water and keep the temperature uniform. Three thermocouples were used to monitor the temperatures of the tank and temperatures before and after the membrane cell. The membrane cell has a tube-shell configuration with feed water flowing through the tubular membrane and the permeate flowing through the glass shell which is exposed to ambient atmosphere. The flow rates of feed water were kept at 1 L/min for all the runs. The effective membrane area was about 20 cm^2. The permeation experiments were conducted at a temperature range of 25 to 95°C and feed side pressure of ambient to 780 kPa. To prevent sample loss through evaporation, permeate samples were collected in an ice cold trap for the runs at temperature above 75°C. Permeate was collected in the vial in order to determine the permeate flux.

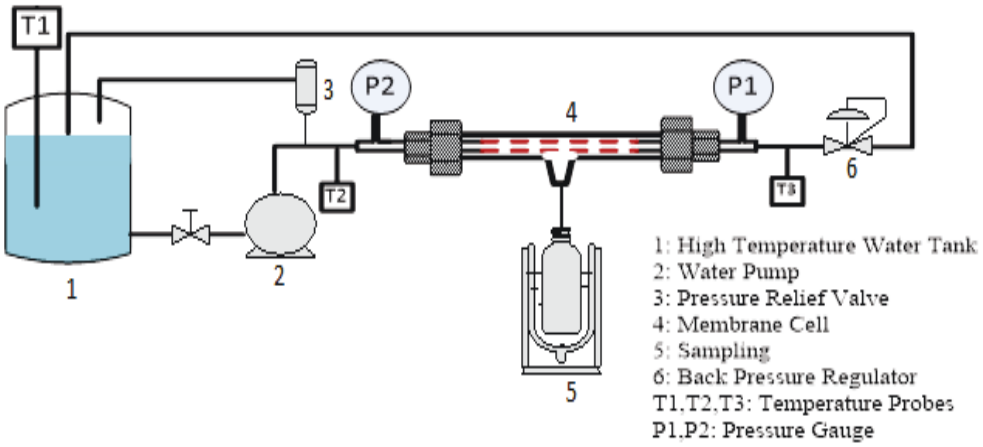

Figure 18. Schematic of low temperature tubular cross-flow membrane system for water purification.

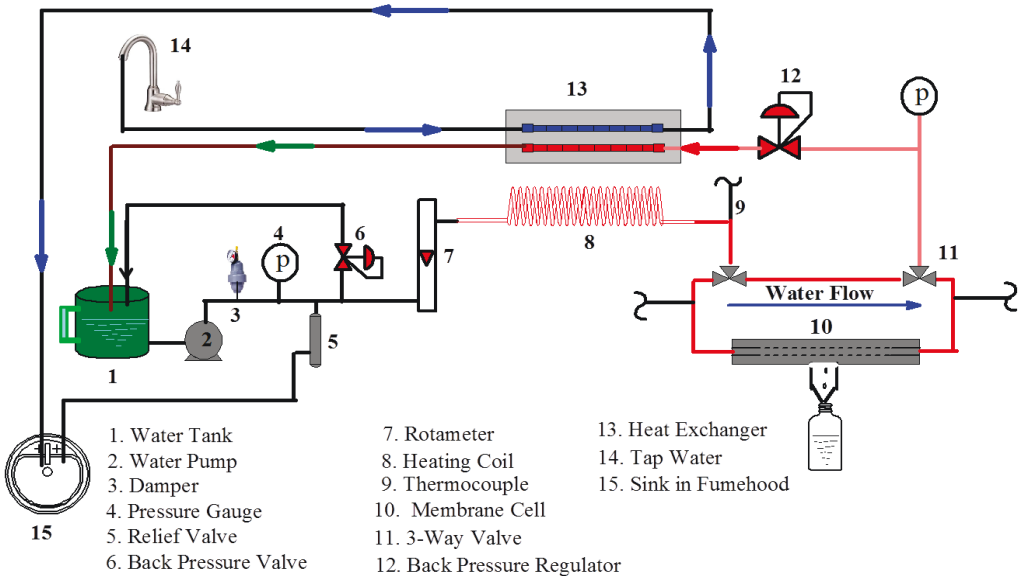

Figure 19. Schematic of high temperature tubular cross-flow membrane test system for water purification.

Figure 19 shows the high temperature system. This system is designed to work at temperatures as high as 160°C to simulate the temperature of SAGD produced water. A coiled tube was placed inside a tubular furnace to increase the water temperature. In the new design, the temperature of circulated water is cooled down by the heat exchanger before returning to the tank to avoid damaging to the pump.

The cooling line of the heat exchanger is connected to the tap water and it was adjusted manually.

The flow rates of feed water were kept at 50 ml/min for all the runs. The effective membrane area was about 20 cm^2. The permeation experiments were conducted at a temperature range of 25 to 160°C and feed side pressure of ambient to 780 kPa.

2.7. Membrane evaluation and analytical methods

The water softening performance of the clinoptilolite composite membranes was evaluated by permeation flux, removal of total and calcium hardness, and reduction of solution conductivity. The following equations were used for calculation of water permeation flux, and hardness removal.

$$\text{Permeate flux} = \frac{W}{A \times t} \tag{2.1}$$

Where W is the weight of the permeate sample in kg, A is the membrane's effective area in m^2, and t is the sample collection time in hours.

$$\text{Total hardness reduction } (\%) = \frac{TTH - PTH}{TTH} \times 100\% \tag{2.2}$$

$$\text{Ca hardness reduction } (\%) = \frac{TCH - PCH}{TCH} \times 100\% \tag{2.3}$$

Where TTH is the total hardness of the tank's water (ppm), PTH is the total hardness (ppm) of the permeate water, while TCH and PCH are the tank's water Ca hardness (ppm) and permeate's Ca hardness (ppm), respectively.

Total and calcium hardness of samples of feed and permeation sides was analyzed by using a water hardness kit (Hach Cat. No. 1457-01) to determine the total hardness based on $CaCO_3$ as well as calcium hardness. Conductivity of the solution was measured by pH-conductivity meter (Accumat XL 20) for both feed and permeate water.

3. Results and Discussion

3.1. Membrane characterization

The zeolite membrane or its components are characterized by SEM, XRD, PSD and permeation/separation tests.

X-ray diffraction (XRD):

XRD patterns of the raw clinoptilolite powder and the composite mixture of clinoptilolite and aluminum phosphate binder after preparation method outlined in section 2.5 of chapter 2 are shown in figure 20. The absence of aluminum and phosphate phases in the XRD profiles suggests that no crystal formation of aluminum phosphate occurred during the heat treatment. Clinoptilolite crystals detected on the surface of the sample suggest that zeolite channels are well exposed on the surface of the composite membrane allowing accessibility to the feed water stream.

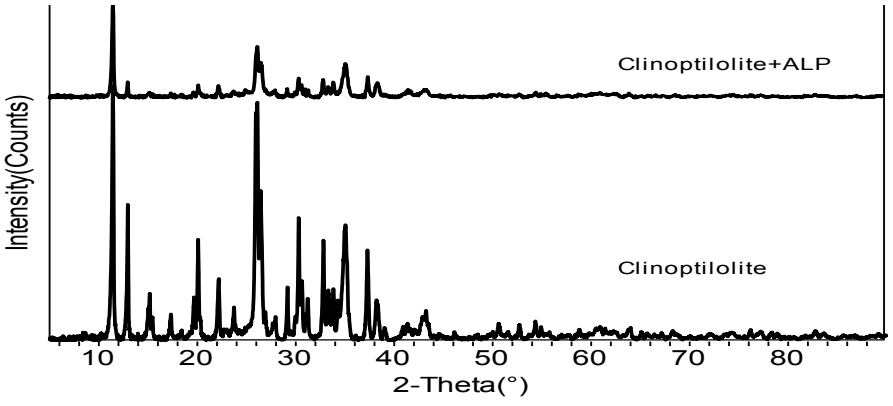

Figure 20. XRD patterns of natural zeolite clinoptilolite powders (St. Cloud, Winston, NM, USA) and the composite coating material of clinoptilolite and aluminum phosphate.

Scanning electron microscopy (SEM):

The back-scattered electron image in figure 21 shows a homogenously milled mixture of clinoptilolite and aluminum phosphate.

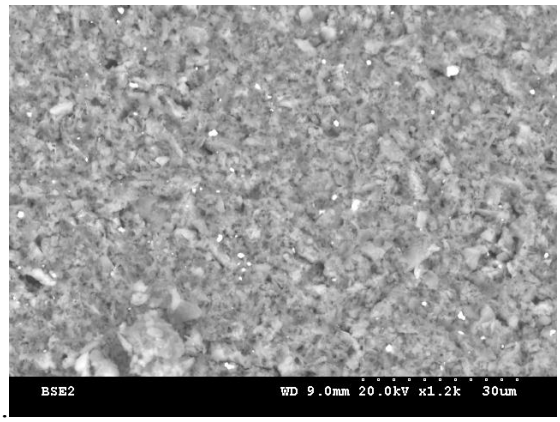

Figure 21. Surface morphology of the clinoptilolite and aluminum phosphate composite taken by SEM.

The cross section of a tubular membrane after testing at 95°C and 780 kPa is shown in figure 22. The clinoptilolite composite coating covers uniformly the surface of the porous substrate, which was pre-coated with TiO_2. The thickness of the TiO_2 layer was about 10µm, while the composite layer was ~60µm. Large cracks can be observed particularly at the interface of the zeolite membrane layers. The cracks could have propagated during the testing process where the membrane layers experience thermal and mechanical stress from heating and applied water pressure. These stresses are later released through formation of cracks at the interface of mechanically bonded zeolite membranes rather than through the rigid metallic support.

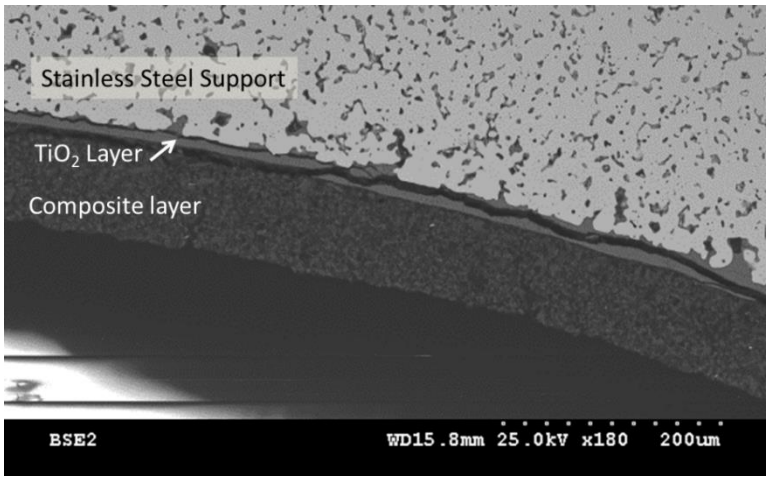

Figure 22. Cross-section of a porous stainless steel tube coated with TiO_2 layer and a composite layer of natural zeolite clinoptilolite in aluminum phosphate binder, after testing at 95°C and 780 kPa.

Particle size distribution (PSD):

Particle size distribution patterns of St. Cloud's Ash Meadows clinoptilolite and two samples of clinoptilolite in water with two methods of mixing are shown in figures 23-25. Sample one: mixed clinoptilolite with method 1 (by stirring).

Sample two: mixed clinoptilolite with method 2 (by ball milling).

In table 5, the distribution of clinoptilolite particle sizes of 10, 50, and 90 percent of the solutions are shown.

Particles were assumed to be spherical by the analysis software with the diameter D50, describing 50% of the particles' sizes. The Ash Meadows clinoptilolite D50 was identified as 12.30 μm, Sample 1 as 5.64, Sample 2 as 5.16.

By comparing particle size distribution of Sample 1 and Sample 2, it is concluded that mixing procedures that are used in this study have no major effect on

reducing the particle sizes, however, the two mixing techniques may mainly affect homogeneous and rheological behavior of the samples.

Table 5. Particle sizes of 10, 50, and 90 percent of the solutions

	D×(10) (µm)	***D×(50) (µm)***	***D×(90) (µm)***
Clinoptilolite powder	2.82	12.30	38.10
Sample 1	1.64	5.64	14.0
Sample 2	1.56	5.16	12.6

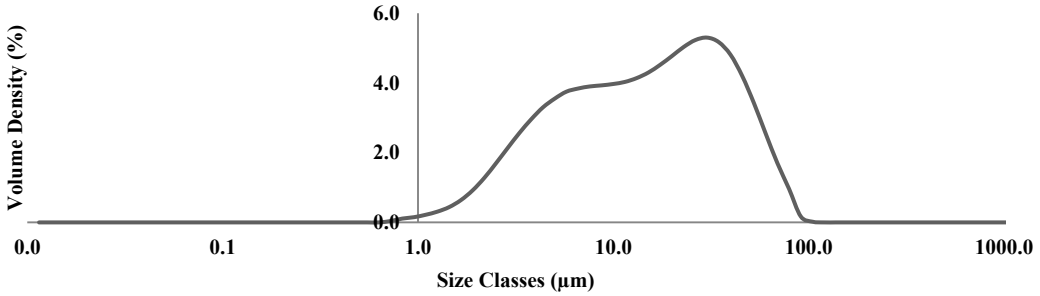

Figure 23. Particle size distribution for Ash Meadows clinoptilolite.

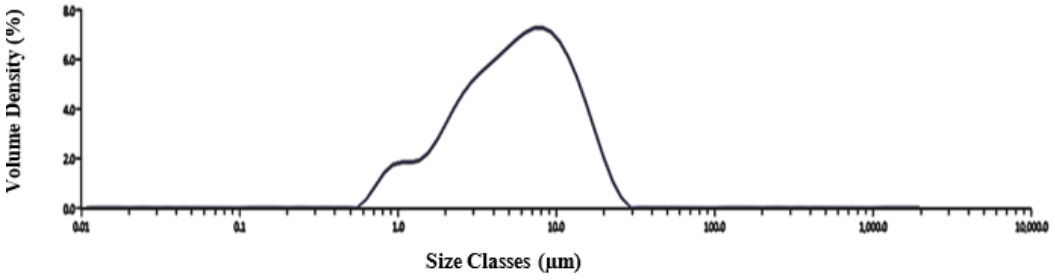

Figure 24. Particle size distribution for Sample one.

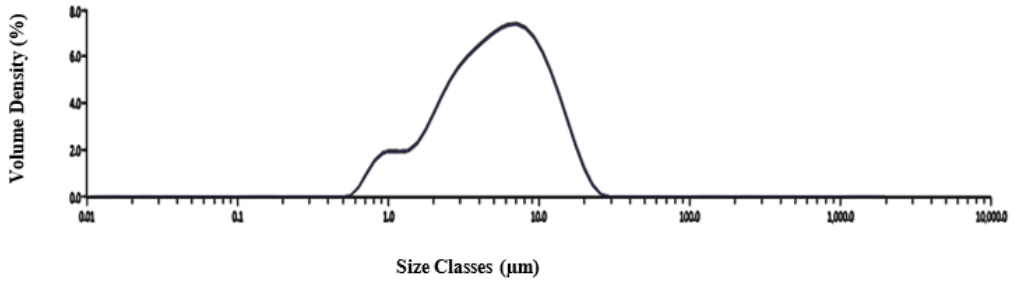

Figure 25. Particle size distribution for Sample two.

3.2. Experimental results of water softening

Water softening tests are conducted for porous stainless steel supported clinoptilolite-aluminum phosphate composite membranes with four different supports' pore sizes of 2, 1, 0.5, and 0.02μm in the temperatures between room temperature and 160°C and from ambient pressure to 780 kPa feed side pressure. The coating materials for all of them were clinoptilolite powders, aluminum phosphate (ALP), and DI water in an equal weight ratio and heat treatment conditions. The effect of different materials mixing procedure, coating procedure, and testing conditions on permeate flux, total hardness, Ca hardness, and conductivity of permeate have been studied.

Clinoptilolite-ALP composite membrane (single or multiple layers) were coated on the inner surface of stainless steel tubular supports. Each tube is tested for at least three days and tap water was used as a source for water softening tests. The tap water quality of city of Edmonton is presented in chapter 2 section 2.4.

Stainless steel tubes with pore size of 0.5 and 0.02µm were pre-coated with 10µm layer of TiO_2 by the manufacturer. This titanium oxide layer acts as an intermediate layer providing both structural and material buffer and transition between the further coated zeolite membrane and porous stainless steel tubular substrate.

The performance of supported clinoptilolite-aluminum phosphate membranes in water softening were evaluated by permeate flux, removal of total and Ca hardness, and conductivity reduction of feed water.

3.2.1. Single layer coated membranes

3.2.1.1. Effect of different supports' pore size on the single layer coated membrane

The experimental results from water softening performed for 1 and 0.5µm tubes at 25°C to 95°C are presented in figures 26-29. Figure 26 shows that water flux through the membrane increases with increasing temperature. The permeate flux obtained at 95°C for tube 1µm and 0.5µm was about 1.7 and 5.7 times higher than the flux at 25°C respectively. Temperature also, has a significant effect on hardness removal and conductivity reduction of the feed water as shown in figures 27-29. Christidis et al. [22] have found that heating can reduce surface area and microporosity of HEU-type zeolites. As temperature increases, zeolitic pores/channels of the clinoptilolite framework contract [91] favoring the size exclusive molecular/ion sieving processes to occur . As the aperture of the zeolite channels decreases, blocking of hydrated Ca and Mg ions by size exclusion increases. Over 21.32% and 6% of the total hardness removal was achieved at 95°C

for tubes with pore sizes of 0.5 and 1µm, respectively. The reduction of conductivity is consistent with the removal of hardness indicating the effective rejection of cations through clinoptilolite molecular/ion sieving. The temperature dependence of water permeation through clinoptilolite composite membrane indicated the permeation is an activated diffusion process.

Because the water flow was under ambient pressure, operating temperature was kept below 95°C to ensure that water in the membrane system was in liquid phase. For tube with pore size of 1µm the system pressure could not be increased over 367 kPa at room temperature and the flux was 3976 kg/m^2.h. For tube 0.5µm the pressure increased to 780kPa in room temperature and the flux was 3926.308 kg/m^2.h. For stainless steel tubes with pore size larger than 0.5µm, the system pressure setup was limited due to the high permeation flux; therefore these membranes were tested at system pressure close to one atmosphere and temperature below 100°C.

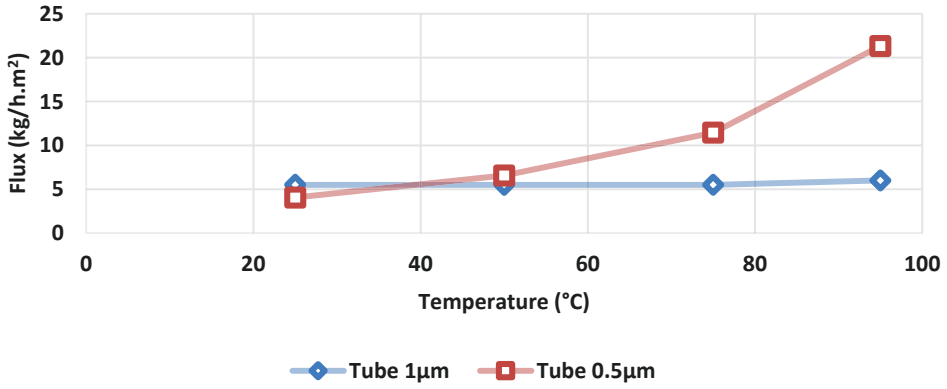

Figure 26. Permeate Water flux through the 1 and 0.5µm metal supported composite clinoptilolite-aluminum phosphate membranes at 25-95°C temperatures and ambient pressure.

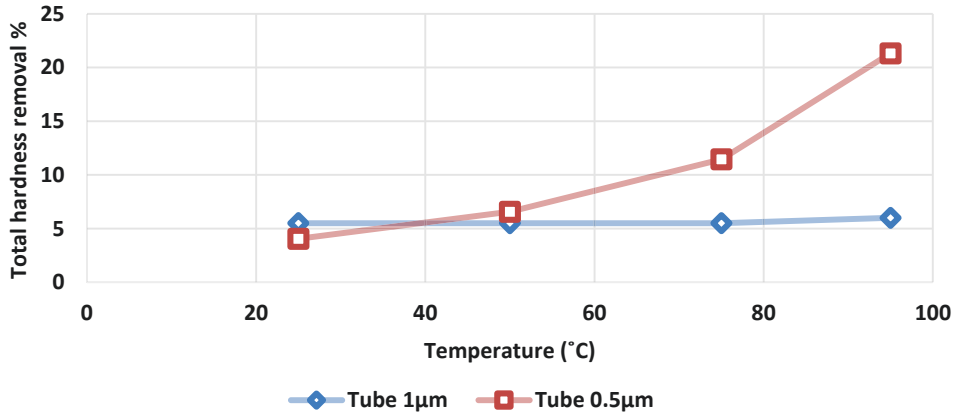

Figure 27. Total hardness reduction through the 1 and 0.5µm metal supported composite clinoptilolite-aluminum phosphate membranes at 25-95°C temperatures and ambient pressure.

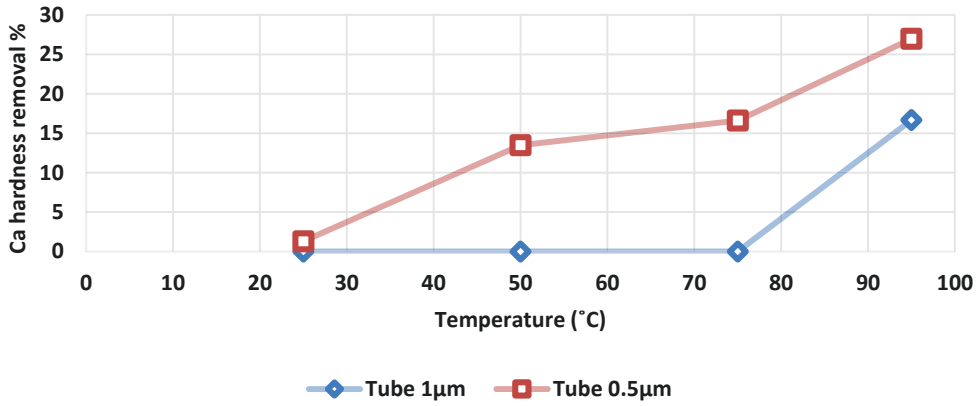

Figure 28. Ca hardness reduction through the 1 and 0.5µm metal supported composite clinoptilolite-aluminum phosphate membranes at 25-95°C temperatures and ambient pressure.

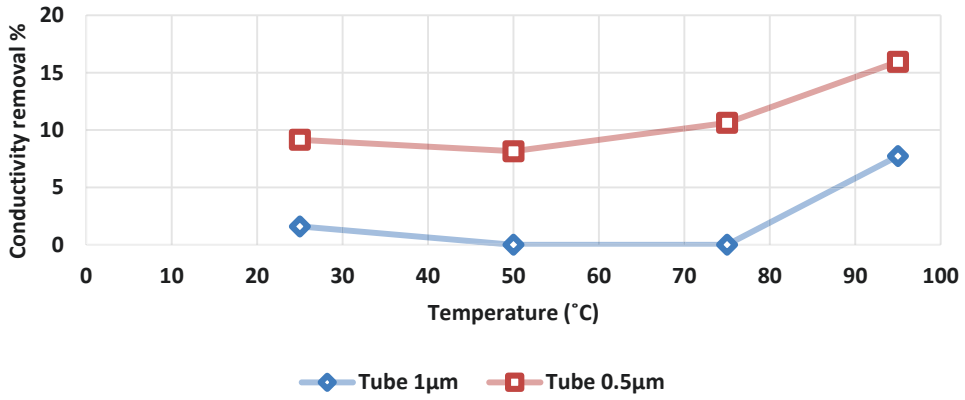

Figure 29. Conductivity reduction through the 1 and 0.5µm metal supported composite clinoptilolite-aluminum phosphate membranes at 25-95°C temperatures and ambient pressure.

3.2.1.2. Effect of feed pressure on the performance of single layer coated membranes

Tube 0.02µm is selected for studying the effect of feed pressure on the performance of membranes. Because feed side pressure can be increased to 780 kPa for only this tube size. For the membranes coated on the substrate tube of 0.02µm pore size, a feed side pressure of above one atmosphere was required to drive water through the membrane to achieve a measurable flux. Therefore, water softening for the tubes of 0.02µm pore size was tested at feed side pressures of 505 and 780 kPa and temperatures from room temperature to 160°C. Experimental results are shown in figures 30-33.

Figure 30 shows effects of feed side pressure on permeate flux of two different 0.02µm tubular membranes. The permeate flux was about 7 times higher at 780 kPa than that at 505 kPa.

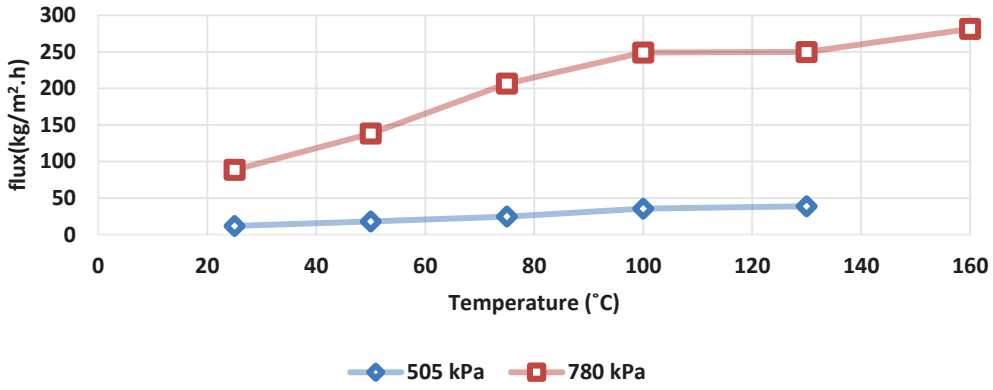

Figure 30. Water flux through the 0.02µm metal supported composite clinoptilolite-aluminum phosphate membranes at 25-160°C temperatures and at 505 and 780 kPa pressures.

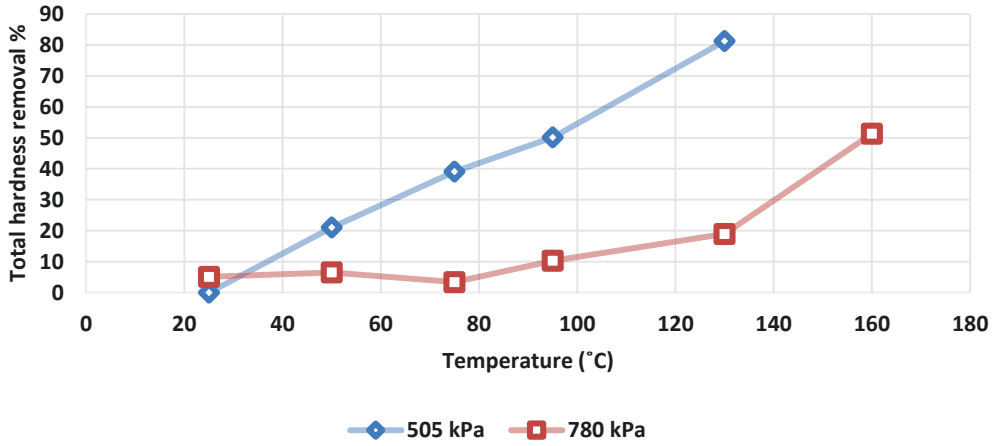

Figure 31. Total hardness reduction through the 0.02µm metal supported composite clinoptilolite-aluminum phosphate membranes at 25-160°C temperatures and at 505 and 780 kPa pressures.

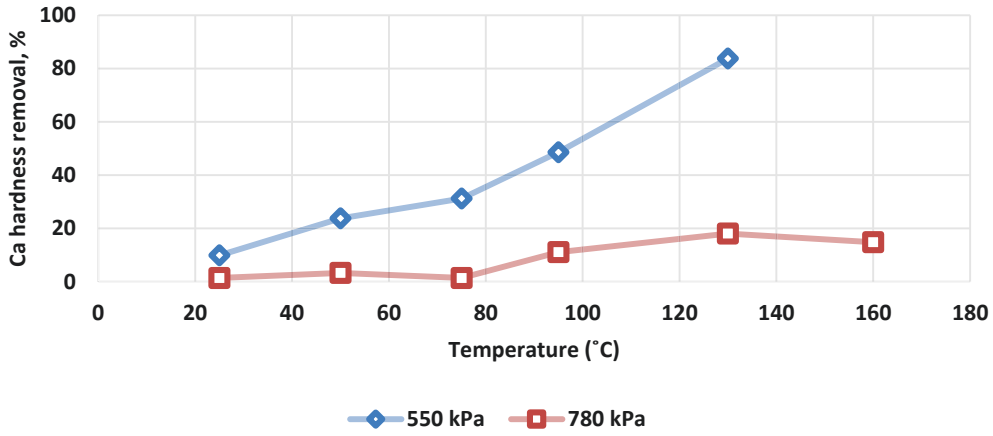

Figure 32. Ca hardness reduction through the 0.02µm metal supported composite clinoptilolite-aluminum phosphate membranes at 25-160°C temperatures and at 505 and 780 kPa pressures.

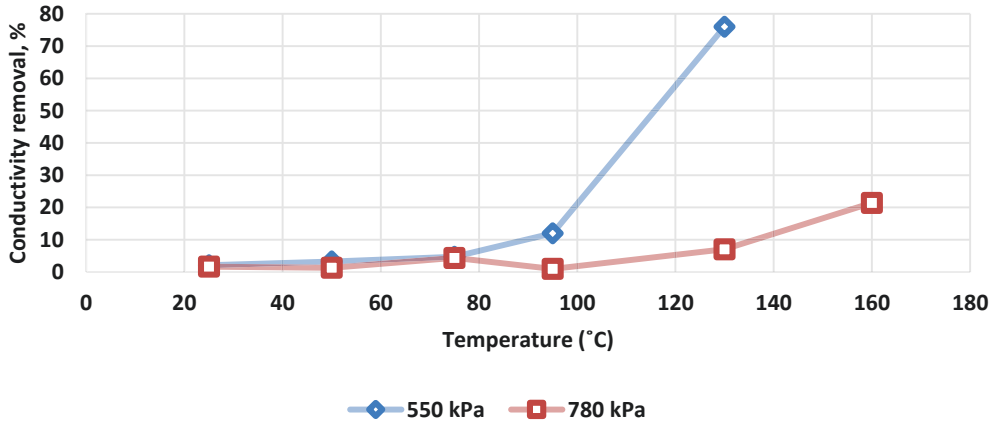

Figure 33. Conductivity reduction through the 0.02µm metal supported composite clinoptilolite-aluminum phosphate membranes at 25-160°C temperatures and at 505 and 780 kPa pressures.

3.2.3.3. Effect of speed of coating in the first layer coating membrane

The effect of different coating procedures on permeate flux are shown in figure 34. These two 0.02µm tubes are same in all coating procedures and just different in speed of coating during the dip coating procedure. They are coated with 1 and 6

ml/min slurry injection speed. As it is mentioned in chapter 2 section 2.5.2, the thickness of the coating layer actually is more sensitive to the draining flow rate than the feeding flow rate. It is shown in figures 34-37 the difference in flux ad total hardness removal between these two tubes is not significant. Which shows that the effect of speed of coating on the performance of membrane is less than other effects that is mentioned in section 2.5.2 such as drain speed which was kept same here for both tubes.

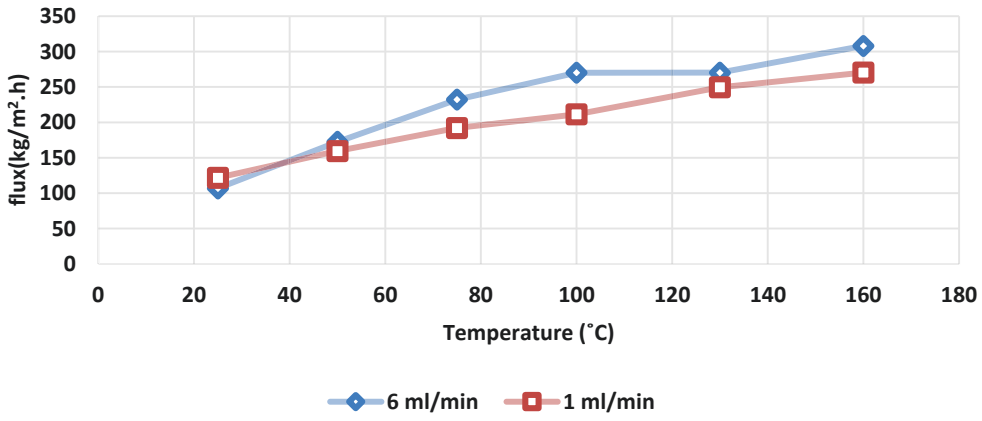

Figure 34. Water flux through the 0.02µm metal supported composite clinoptilolite-aluminum phosphate membranes with different in speed of coating at 25-160˚C temperatures and 780 kPa pressure.

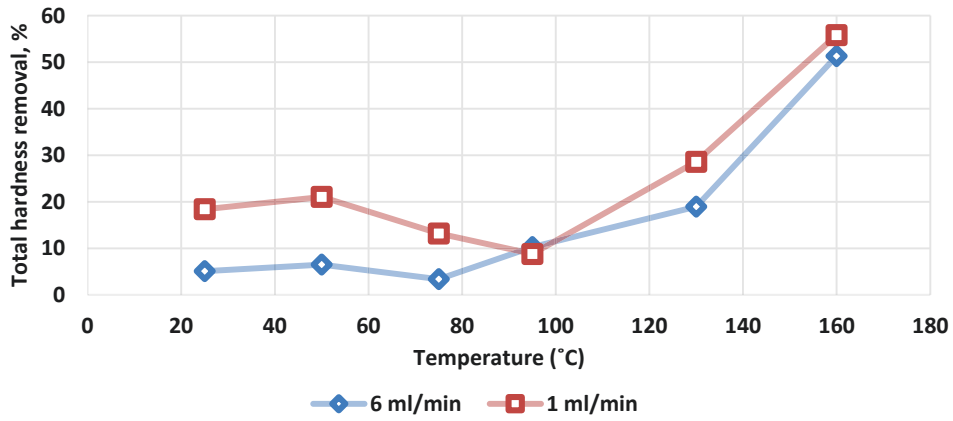

Figure 35. Total hardness removal through the 0.02µm metal supported composite clinoptilolite-aluminum phosphate membranes with different in speed of coating at 25-160˚C temperatures and 780 kPa pressure.

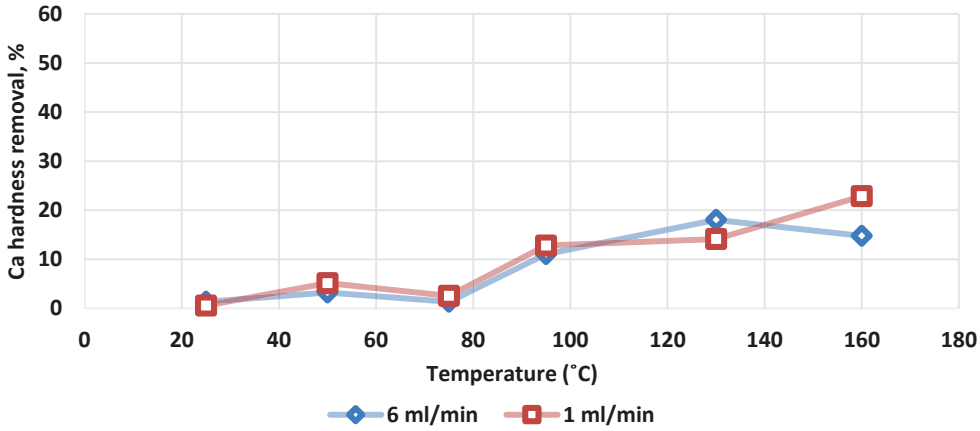

Figure 36. Ca hardness removal through the 0.02µm metal supported composite clinoptilolite-aluminum phosphate membranes with different in speed of coating at 25-160˚C temperatures and 780 kPa pressure.

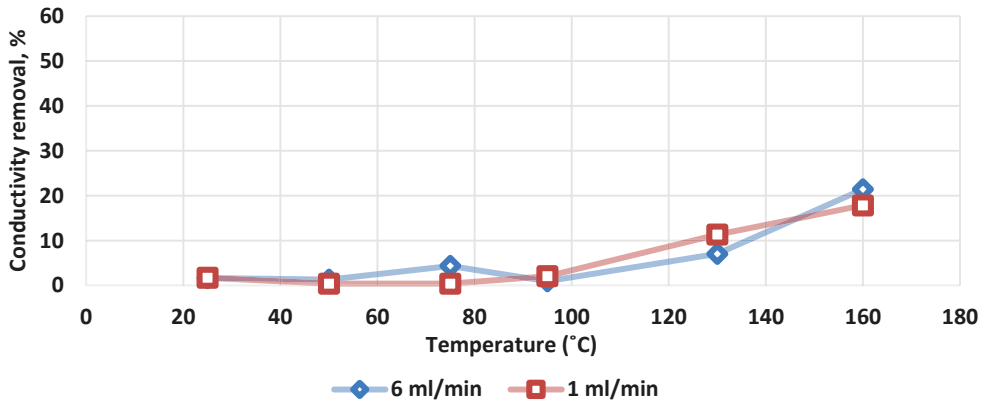

Figure 37. Conductivity reduction through the 0.02µm metal supported composite clinoptilolite-aluminum phosphate membranes with different in speed of coating at 25-160˚C temperatures and 780 kPa pressure.

3.2.3.4. Summary of single layer coated membranes

Experiment results from single layer coated stainless steel tubular membrane showed improvement of membrane performance as compared to non-coated support. First layer coated membrane performance is summarized in figures 38 and 39.

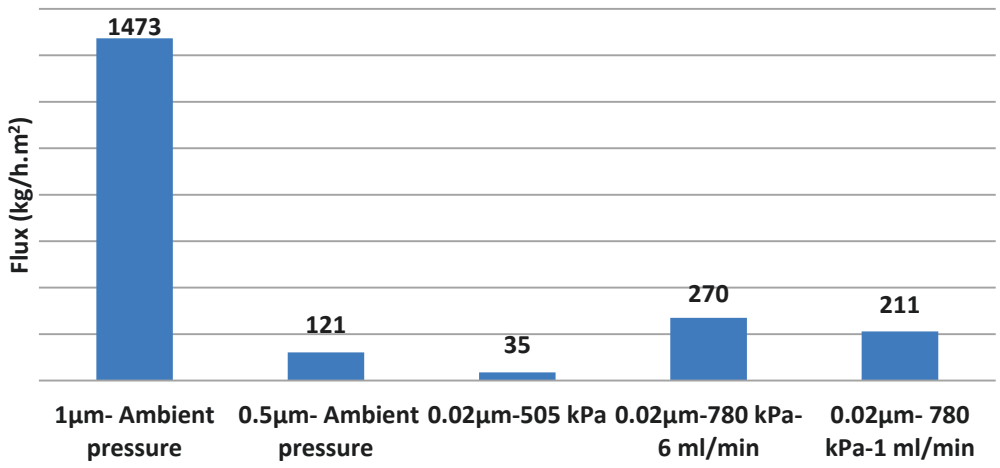

Figure 38. Permeate flux through five different tubes with one layer coated membrane at 100°C.

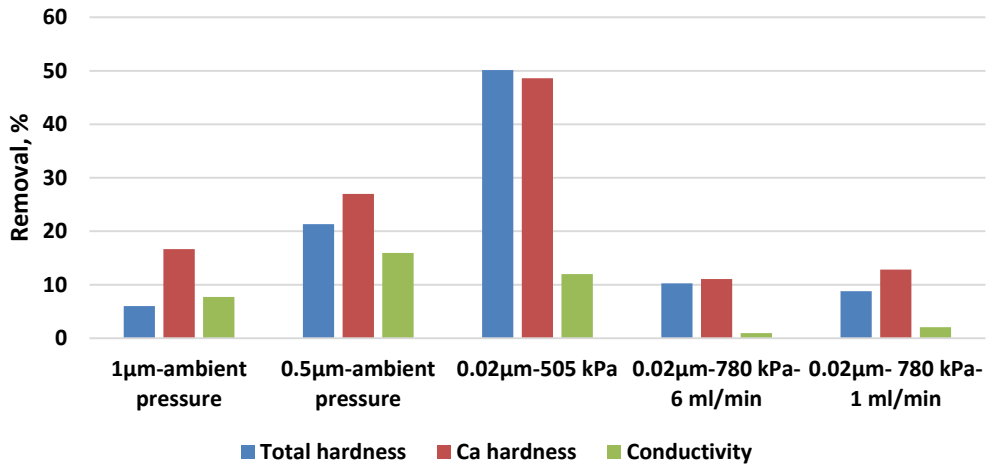

Figure 39. Total hardness, Ca hardness, and conductivity reduction through five different tubes with one layer coated membrane at 100°C.

Figure 38 shows that flux for tube 1µm is the highest flux that obtained from one layer coated membranes at 100°C, while membranes 1 and 0.5µm are tested in ambient pressures which are not practicable for temperatures higher than 100°C. In addition, it is shown in figure 39 that tube 0.02µm that was tested under 505 kPa feed side pressure had more hardness and conductivity reduction than the one was tested under 780 kPa. Tubes 1 and 0.02µm were further coated for the second time to improve water softening performances. First layer coated membrane on tube 2 µm was not fully covered the large pores of tube, so the second layer applied on. The results of the second layer coated membranes are explained in the next section.

3.2.2. Double layer coated membranes

Single layer coated stainless steel tubular substrates with three different pore sizes of 2, 1 and 0.02µm were further coated to improve water softening performances.

Before applying the next layer the surface of first layer coating was partially removed and roughed, then the tubes were washed in an ultrasonic bath for about 30 minutes and dried in the oven at 70°C for half an hour.

3.2.2.1. Effect of removing/not removing first layer of coating before applying the second layer on membrane performance

For the stainless steel tubular substrates with pore size of 2µm, the second layer of clinoptilolite–ALP composite was coated (a) directly on the first layer and (b) on the surface of removed first layer, respectively. Water softening tests were conducted under feed side pressure of one atmosphere and temperatures up to 95°C due to the difficulty of maintaining high feed side pressure caused by the relatively high permeation flux.

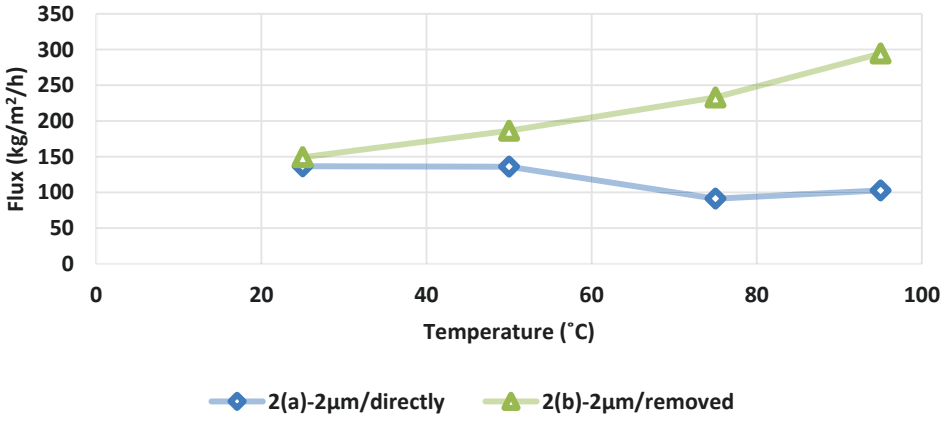

Figure 40. Permeate flux through the two 2µm metal supported composite clinoptilolite-aluminum phosphate membranes at 25-160°C temperatures and 780 kPa pressure. Second layer (a) directly on the first layer (b) on the surface of removed first layer.

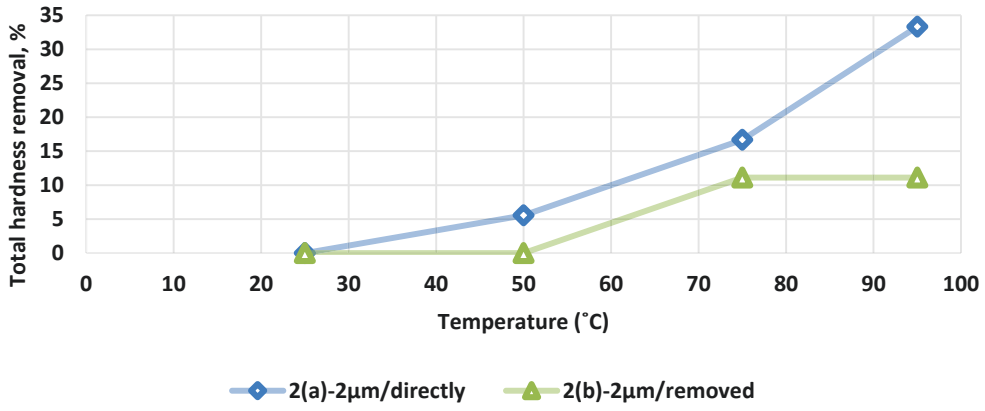

Figure 41. Total hardness removal of two 2µm metal supported composite clinoptilolite-aluminum phosphate membranes at 25-160°C temperatures and 780 kPa pressure. Second layer (a) directly on the first layer (b) on the surface of removed first layer.

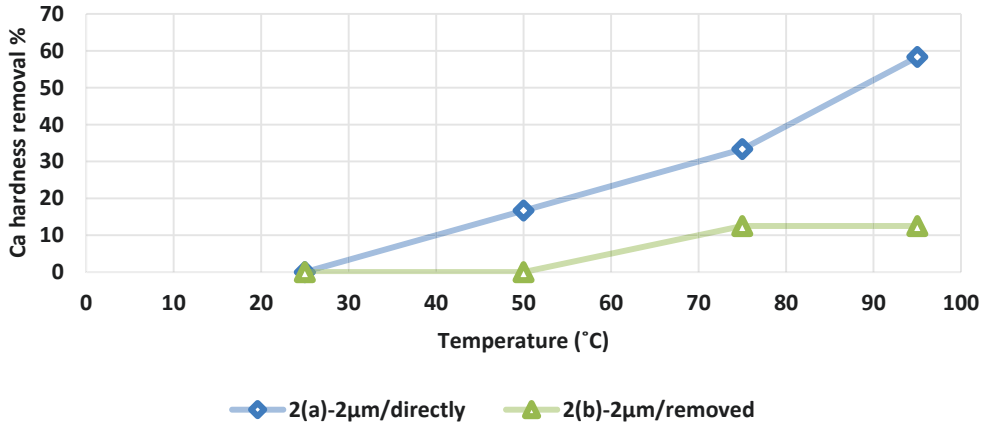

Figure 42. Ca hardness removal of two 2µm metal supported composite clinoptilolite-aluminum phosphate membranes at 25-160°C temperatures and 780 kPa pressure. Second layer (a) directly on the first layer (b) on the surface of removed first layer.

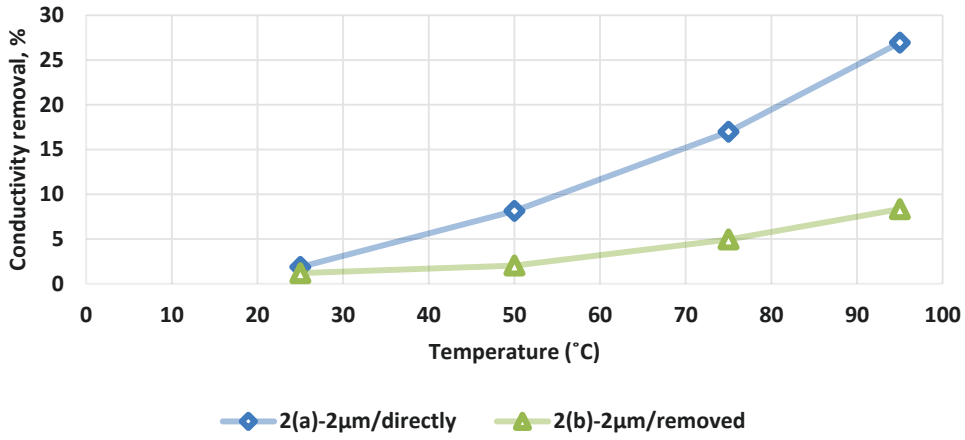

Figure 43. Conductivity reduction of two 2µm metal supported composite clinoptilolite-aluminum phosphate membranes at 25-160°C temperatures and 780kPa pressure. Second layer (a) directly on the first layer (b) on the surface of removed first layer.

As it is shown in figure 40, The permeate flux obtained at 95°C for tube (a) and (b) was 102.7 and 294.4 kg/m^2.h, respectively. Removal of first layer before coating the second layer increased the water flux to about two times. Same as the first layer coated tubes, temperature has a significant effect on hardness removal and conductivity reduction of the feed water as shown in figures 41-43. As temperature increased both water hardness and conductivity were dramatically reduced. Over 58.33% and 12.5% of the Ca hardness removal was achieved at 95°C for tube (a) and (b), respectively. The lower permeation flux of the directly coated second layer tubular membrane was corresponded to a better water softening performance in terms of more efficient hardness removal and conductivity reduction. These results demonstrated that directly coated second layer of clinoptilolite-ALP composite membrane has less defects and better sealing of the larger pore in the substrate.

This experiment was repeated for tube 1, and 0.02µm. But, by coating the second layer directly on the first layer, the membrane became too dense to have a permeate flux in the lab conditions. So for tube 1 and 0.02µm partially removal of first layer benefit the performance.

3.2.2.2. Effect of two different mixing techniques

The performances of clinoptilolite-ALP composite coated tubular membrane are closely related the pore size, surface chemistry (TiO_2 pre-coated or not) of the substrates and the number of coating layers. Among the substrate with different pore size, single layer coated tubular substrate with a small pore size of 0.02µm showed the best water softening results. Therefore more efforts were made to improve the overall performance of single layer coated 0.02µm tubular membranes. For comparing the mixing procedure of the coating slurry in separation/permeation tests three different 0.02µm tubes are tested. These three 0.02µm tubes are same in all membrane preparation processes and just different in material mixing process. As it is mentioned in chapter 2 section 2.5.1, two methods are used in preparing the coating slurry.

Method 1: ALP and DI water mixed together for about 30 minutes to 1 hour by stirring at 350 rpm. And in the second step, Clinoptilolite powder was added to the mixture and stirred at 700 rpm for about 2-3 hours.

Method 2: three ingredients of coating slurry were mixed by a planetary ball milling at 300 rpm for 20 minutes.

Table 6 describes the mixing methods used for each coating layer of the three 0.02µm tubes.

For tube number 3, due to the permeation flux of 0.73 kg/m^2.h the separation tests could not be completed. The effect of different coating procedure on permeate flux, total harness, Ca hardness and conductivity for tubes number 1 and 2 are shown in figures 44-47.

Tube #1 is tested with low temperature set-up which is mentioned in chapter 2 section 2.6, and Tube #2 is tested with high temperature set-up.

Table 6. Different mixing procedure for three 0.02µm tubes

Tube I.D	***Coating one***	***Coating two***
1	Method 2	Method 2
2	Method 2	Method 1
3	Method 1	Method 1

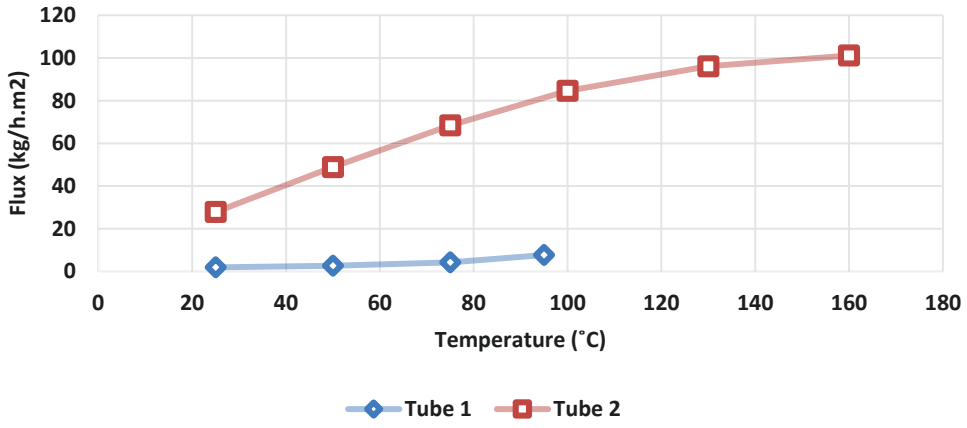

Figure 44. Permeate flux through the two 0.02µm metal supported composite clinoptilolite-aluminum phosphate membranes with different mixing procedure at 25-160°C temperatures and 780 kPa pressures.

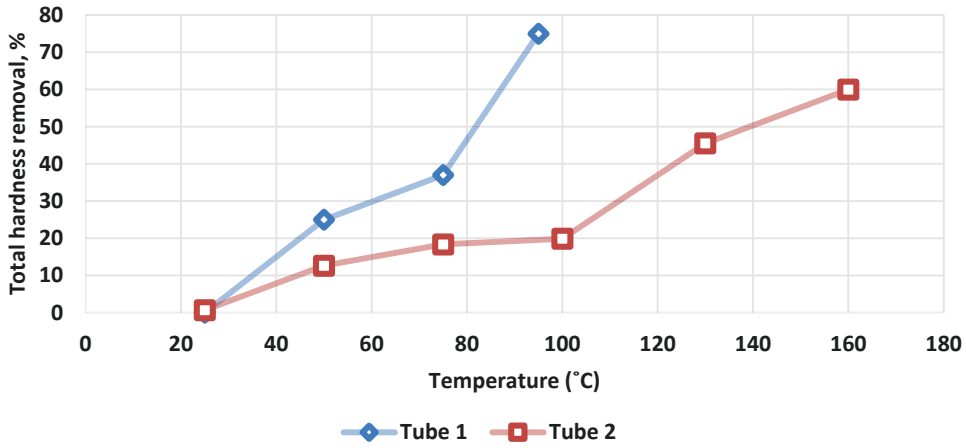

Figure 45. Total hardness removal through the two 0.02µm metal supported composite clinoptilolite-aluminum phosphate membranes with different mixing procedure at 25-160°C temperatures and 780 kPa pressures.

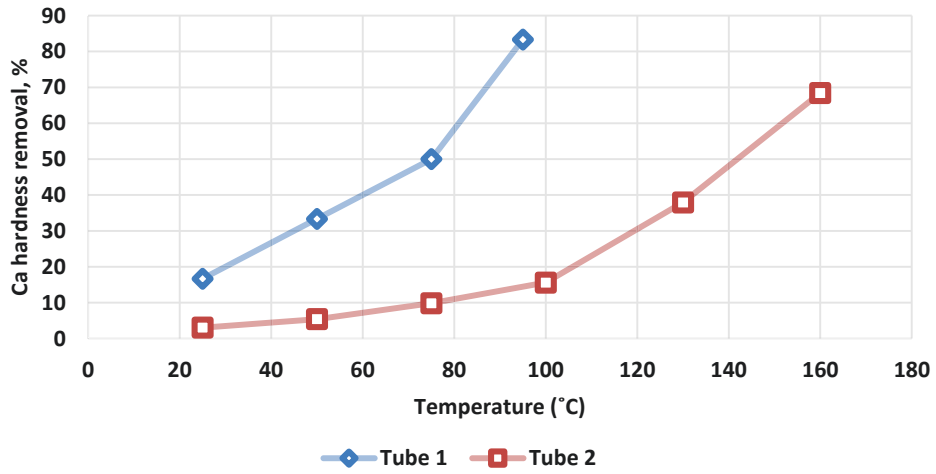

Figure 46. Ca hardness removal through the two 0.02µm metal supported composite clinoptilolite-aluminum phosphate membranes with different mixing procedure at 25-160°C temperatures and 780 kPa pressures.

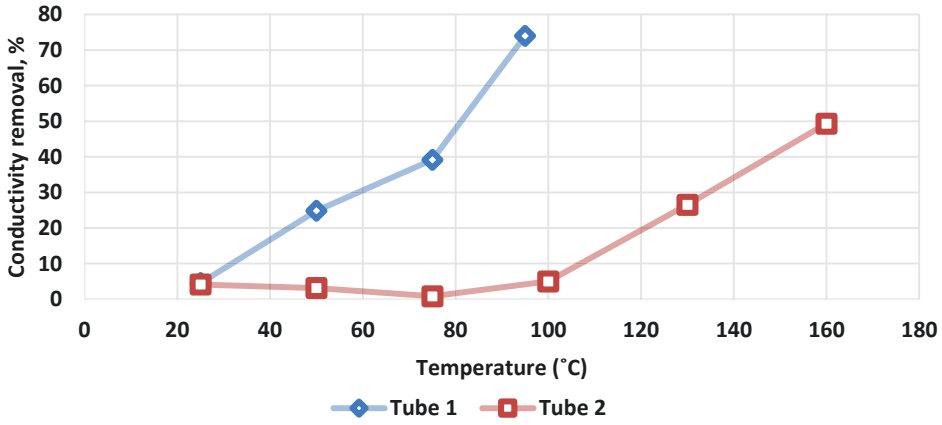

Figure 47. Conductivity reduction through the two 0.02µm metal supported composite clinoptilolite-aluminum phosphate membranes with different mixing procedure at 25-160°C temperatures and 780 kPa pressures.

Experimental results for tube #1 and #2 from figures 44-47 show a high water flux of 7.7 and 84 kg/m^2.h and 75% and ~20% reduction of hardness in a once-through membrane process at 95°C and feed pressure of 780 kPa, respectively. Besides, experimental results for tube #2 from figures 39-42 show a high water flux of

101.17 kg/m^2.h and 59.98% reduction of hardness and conductivity in a once-through membrane process at 160°C and feed pressure of 780 kPa.

In figure 48 these two tubes are compared in terms of permeate flux, total hardness reduction, Ca hardness reduction, and conductivity reduction at ~100°C. It is shown that water softening performance of tube 1 is more than tube 2, and it is because of their difference in their coating slurry mixing methods. As it is explained in section 3.1 two mixing techniques may mainly affect homogeneous and rheological behavior of the samples that is effected in the membrane performance.

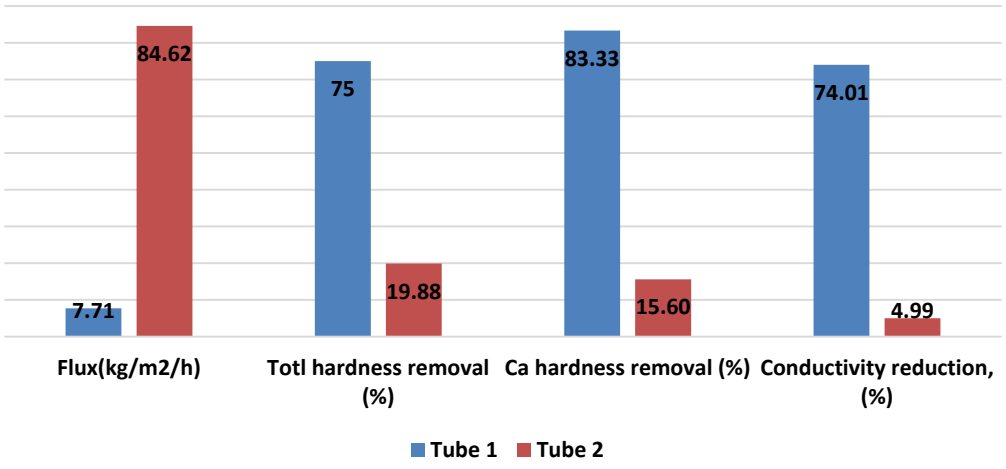

Figure 48. Permeate flux, total hardness reduction, Ca hardness reduction, and conductivity reduction at 95°C for tube #1 and 100°C for tube #2.

By comparing all types of tubes for the first layer and second layer of coating it is concluded that tubes with pore size of 0.02µm with 10µm TiO_2 intermediate layers showed the best results as compared to 2, 1, and 0.5µm tubes. Among 0.02µm tubes, tube #1 had the best results of 75% reduction of hardness, 83.33% Ca hardness and 74.01% conductivity in a once-through membrane process at 95°C

and feed pressure of 780 kPa. Results from Tube #2 showed high water permeation flux, however the lower hardness/conductivity reductions indicated the existence of non-selective pore defects. Therefore, Tube #2 is coated for the third time to reach higher removal of hardness and conductivity in the once-through membrane process.

3.2.3. Triple layer coated membranes

Tube #2 was coated again with the same weight ratio of clinoptilolite powders, ALP, and DI water which were mixed together by stirrer and coated inside the stainless steel support tube.

Table 7. All three coating methods of tube #2.

Tube I.D	*Coating 1*	*Coating 2*	*Coating 3*
2	Method 2	Method 1	Method 1

The experimental results from water softening performed for tube #2 at 25°C to 160°C temperature and 780 kPa pressures for all three coating layers are presented in figures 49-52. Each layer of membrane was tested for three days. For the first two layers all days of testing were in a row, but for third layer the first two days was in a row and the third day was tested after a month.

The dramatic changes in ion rejections are observed after 100°C in figures 50-52. The water change from liquid-phase to vapor-phase after 100°C. The 780 kPa pressure is applied to the system for preventing this phenomena to happen, but the pressure on the other side of membrane is the ambient pressure. Then, the membrane acts like a barrier between liquid-phase and vapor-phase. So, we have a

pervaporation and molecular sieving together as temperature passes 100°C. The same pressure (780 kPa) on the other side of the membrane should be applied to prevent pervaporation in the system.

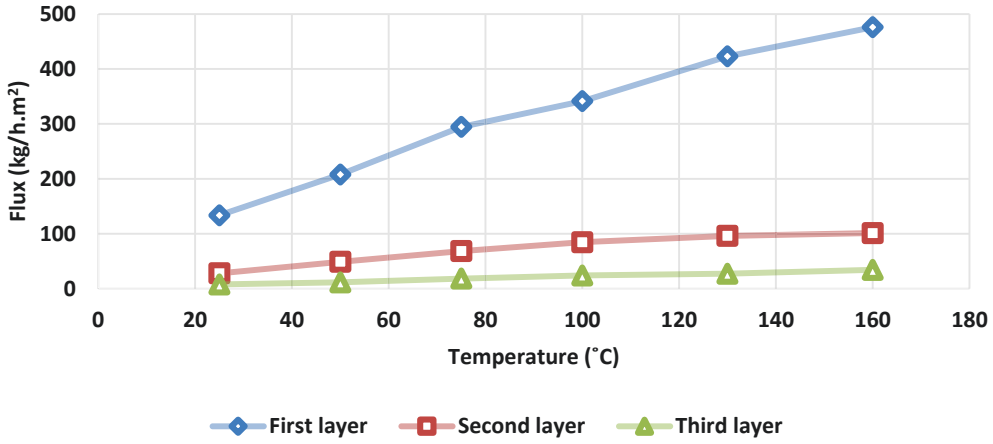

Figure 49. Permeate flux through the 0.02µm metal supported composite clinoptilolite-aluminum phosphate membranes for three membrane layers at 25-160°C temperatures and 780 kPa pressures.

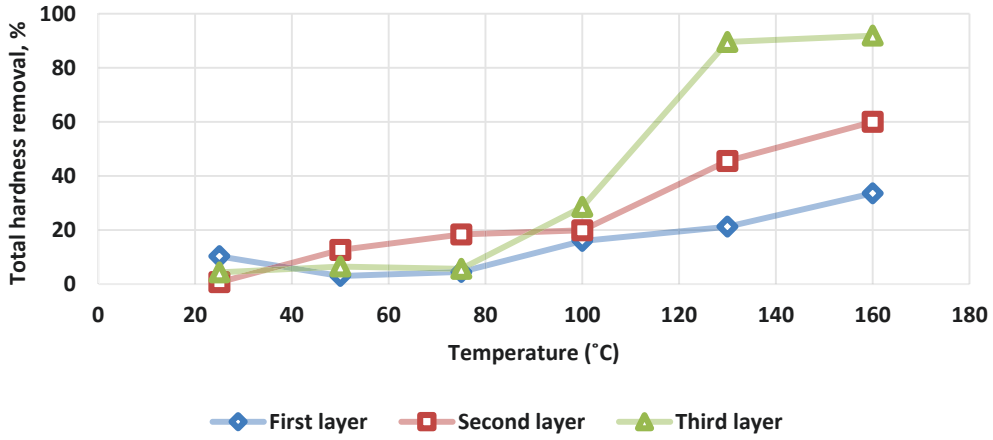

Figure 50. Total hardness removal through the 0.02µm metal supported composite clinoptilolite-aluminum phosphate membranes for three membrane layers at 25-160°C temperatures and 780 kPa pressures.

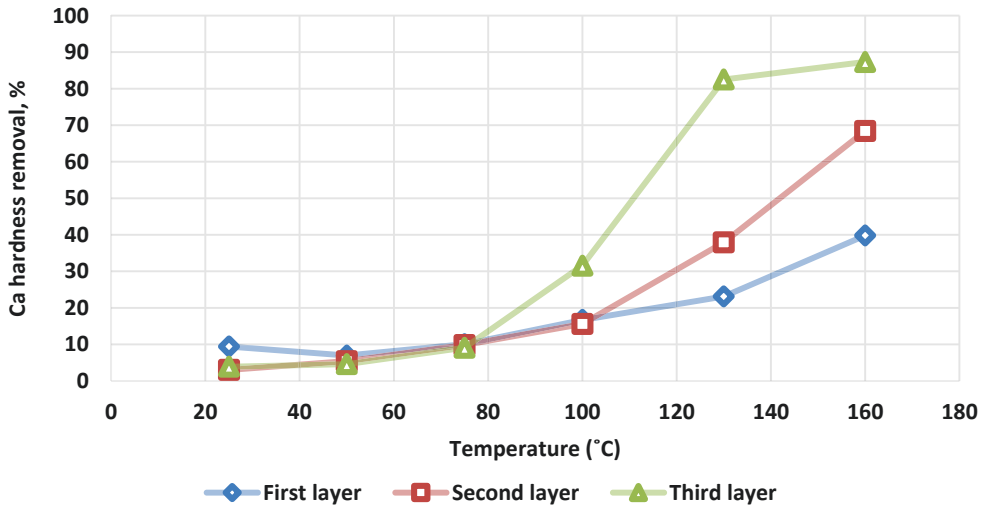

Figure 51. Ca hardness removal through the 0.02µm metal supported composite clinoptilolite-aluminum phosphate membranes for three membrane layers at 25-160°C temperatures and 780 kPa pressures.

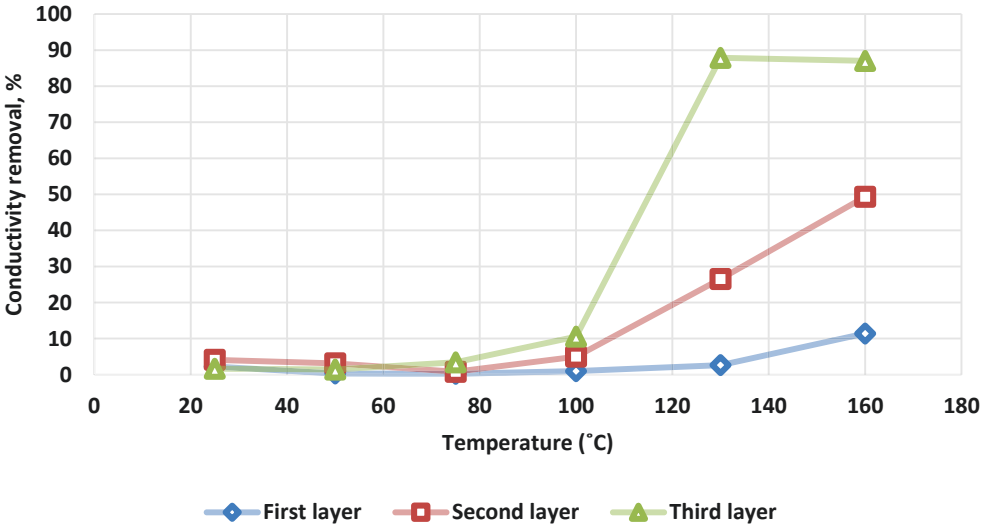

Figure 52. Conductivity reduction through the 0.02µm metal supported composite clinoptilolite-aluminum phosphate membranes for three membrane layers at 25-160°C temperatures and 780 kPa pressures.

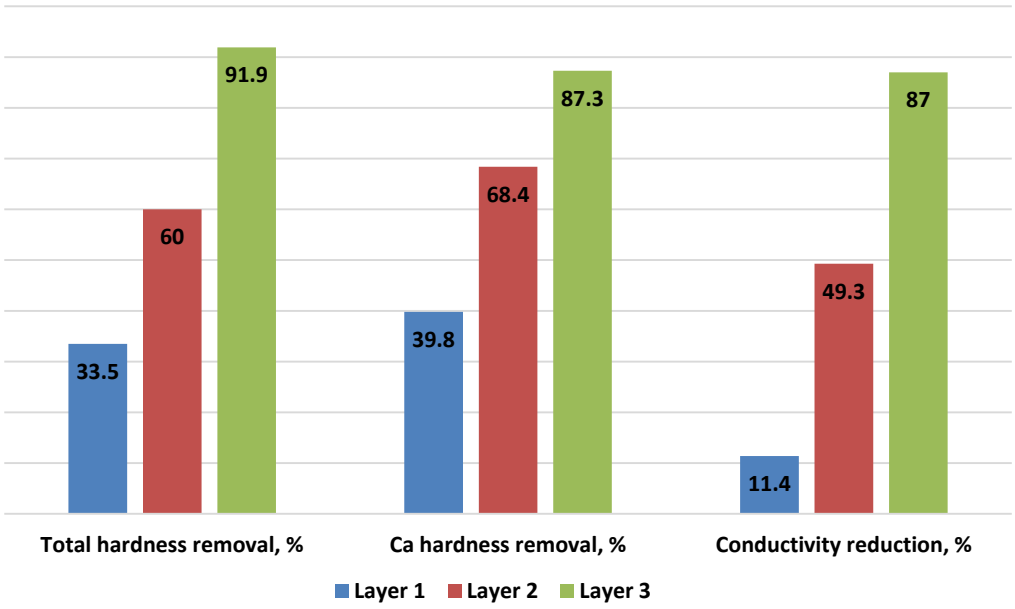

Figure 53. Total hardness, Ca hardness, and conductivity removal through the 0.02µm metal supported composite clinoptilolite-aluminum phosphate membrane for three membrane layers at 160°C temperatures and 780 kPa pressures.

As it is shown in figure 54 although the third day of testing is done after about one month the results are still consistent with the results obtained in the first two days indicating the clinoptilolite-ALP composite membrane coating is stable both chemically and physically under the testing conditions.

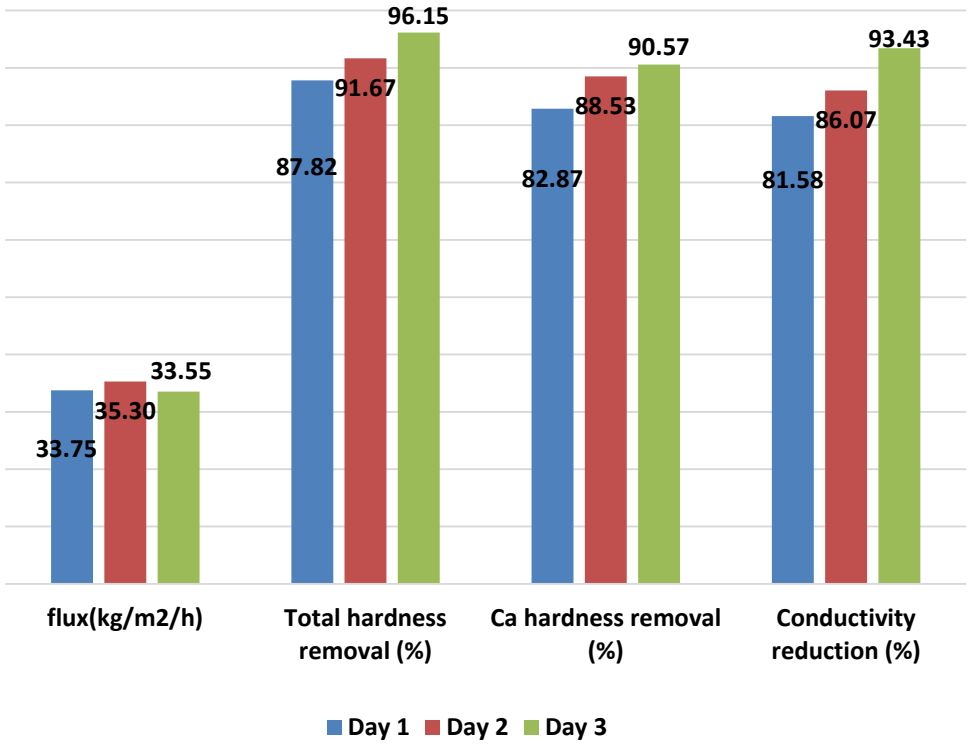

Figure 54. Reproducibility tests at 160°C temperature and 780 kPa pressure.

4. Conclusions

Water or/and produced water treatment technology is more efficient when the treatment unit is a compact system of pre-treatment, membrane, and post treatment. Membrane technology for water softening is one of the most promising technology for the final water quality requirements. Working life time, fouling, scaling, final cost, availability of membrane material, and permeate quality and flux are challenges for membrane technology which are under study for several years. In order to recycle/reuse produced water from oil sands SAGD process, membrane materials not only must be able to selectively remove mineral ions, oil contaminants and fine particles, but also be chemically and thermally stable to withstand the harsh water conditions.

Clinoptilolite as a membrane material is a good candidate for working under the harsh conditions. In this thesis work, natural zeolite clinoptilolite composite coated stainless steel tubular membrane was developed for water desalination and potential application for oil sands SAGD water treatment. Experimental results from this study showed that high water flux of 34.20 $kg/m^2.h$ and high hardness removal of 91.88% can be achieved by the coated stainless steel tubular membrane from Edmonton tap water under simulated SAGD water temperature and pressure. Lower cation rejection observed at room temperature suggests that some defects existed in the fabricated membranes.

In conclusion, the promising results reported in this study show that using low cost natural clinoptilolite composite coated stainless steel tubular membrane for water

softening, desalination and potential application for oil sands SAGD water treatment is a very practical approach to the water issue in the oil and oil sands industries.

Bibliography

[1] P. D. Swenson, "Natural zeolite membranes for gas and liquid separations," University of Alberta, 2012.

[2] C. C. H. Lin, K. A. Dambrowitz, and S. M. Kuznicki, "Evolving applications of zeolite molecular sieves," *Can. J. Chem. Eng.*, vol. 90, no. 2, pp. 207–216, Apr. 2012.

[3] F. A. Mumpton, *Mineralogy and Geology of natural zeolites*. Mineralogical Society of America, 1977.

[4] T. W. Wang, Ed., *Handbook of Zeolites: structure, properties and applications*. Nova Science Pub Inc, 2009.

[5] Heavy Metal Detox Reviews, "http://www.heavymetaldetoxreview.com/." .

[6] D. W. Breck, *Zeolite Molecular Sieves: Structure, Chemistry, and Use.* USA, 1984.

[7] A. Dyer, *An Introduction to Zeolite Molecular Sieves.* Great Britain: John Wiley & Sons Ltd., 1988.

[8] D. W. Breck, *Zeolite Molecular Sieves: Structure, Chemistry and Use*. New York, NY: Wiley & Sons, Inc, 1974.

[9] D. Mohan and C. U. Pittman, "Arsenic removal from water/wastewater using adsorbents--A critical review.," *J. Hazard. Mater.*, vol. 142, no. 1–2, pp. 1–53, Apr. 2007.

[10] N.-Q. Feng and G.-F. Peng, "Applications of natural zeolite to construction and building materials in China," *Constr. Build. Mater.*, vol. 19, no. 8, pp. 579–584, Oct. 2005.

[11] S. Ko, P. D. Fleming, M. Joyce, and P. Ari-Gur, "High performance nano-titania photocatalytic paper composite. Part II: Preparation and characterization of natural zeolite-based nano-titania composite sheets and study of their photocatalytic activity," *Mater. Sci. Eng. B*, vol. 164, no. 3, pp. 135–139, Oct. 2009.

[12] R. Egashira, S. Tanabe, and H. Habaki, "Adsorption of heavy metals in mine wastewater by Mongolian natural zeolite," *Procedia Eng.*, vol. 42, no. August, pp. 49–57, Jan. 2012.

[13] A. Z. Woinarski, G. W. Stevens, and I. Snape, "A Natural Zeolite Permeable Reactive Barrier to Treat Heavy-Metal Contaminated Waters in

Antarctica," *Process Saf. Environ. Prot.*, vol. 84, no. 2, pp. 109–116, Mar. 2006.

[14] T. Motsi, N. a. Rowson, and M. J. H. Simmons, "Adsorption of heavy metals from acid mine drainage by natural zeolite," *Int. J. Miner. Process.*, vol. 92, no. 1–2, pp. 42–48, Jul. 2009.

[15] A. A. Zorpas, T. Constantinides, A. G. Vlyssides, I. Haralambous, and M. Loizidou, "Heavy metal uptake by natural zeolite and metals partitioning in sewage sludge compost," *Bioresour. Technol.*, vol. 72, pp. 113–119, 2000.

[16] G. Blanchard, M. Maunaye, and G. Martin, "Removal of heavy metals from waters by means of natural zeolites," *Water Res.*, vol. 18, no. 12, pp. 1501–1507, 1984.

[17] E. H. Borai, R. Harjula, L. Malinen, and A. Paajanen, "Efficient removal of cesium from low-level radioactive liquid waste using natural and impregnated zeolite minerals.," *J. Hazard. Mater.*, vol. 172, no. 1, pp. 416–22, Dec. 2009.

[18] M. P. Bernal and J. M. Lopez-Real, "Natural zeolites and sepiolite as ammonium and ammonia adsorbent materials," *Bioresour. Technol.*, vol. 43, no. 1, pp. 27–33, Jan. 1993.

[19] M. Kanyılmaz, N. Tekelioğlu, H. Sevgili, R. Uysal, and a. Aksoy, "Effects of dietary zeolite (clinoptilolite) levels on growth performance, feed utilization and waste excretions by gilthead sea bream juveniles (Sparus aurata)," *Anim. Feed Sci. Technol.*, Oct. 2014.

[20] M. Reháková, S. Čuvanová, M. Dzivák, J. Rimár, and Z. Gaval'ová, "Agricultural and agrochemical uses of natural zeolite of the clinoptilolite type," *Curr. Opin. Solid State Mater. Sci.*, vol. 8, no. 6, pp. 397–404, Dec. 2004.

[21] H. Ghobarkar, O. Schäf, and U. Guth, "Zeolites - from kitchen to space," *Prog. Solid State Chem.*, vol. 27, pp. 29–73, Jan. 1999.

[22] G. Christidis, "Chemical and thermal modification of natural HEU-type zeolitic materials from Armenia, Georgia and Greece," *Appl. Clay Sci.*, vol. 24, no. 1–2, pp. 79–91, Nov. 2003.

[23] D. Zhao, K. Cleare, C. Oliver, C. Ingram, D. Cook, R. Szostak, and L. Kevan, "Characteristics of the synthetic heulandite-clinoptilolite family of zeolites," *Microporous Mesoporous Mater.*, vol. 21, no. 4–6, pp. 371–379, May 1998.

[24] A. Arcoya, J. A. Gonzalez, N. Travieso, C. D. I. Qufmica, and L. Habana, "PHYSICOCHEMICAL AND CATALYTIC PROPERTIES A MODIFIED NATURAL CLINOPTILOLITE," *Clay Miner.*, vol. 29, pp. 123–131, 1994.

[25] G. Gottardi and E. Gallim, *Natural Zeolites*. Germany, Springer-Verlag Berlin,Heidelberg, 1985.

[26] W. T. Schaller and U. S. Geological, "THE MORDENITE-PTILOLITE GROUP; CLINOPTILOLITE, A NEW SPECIES," *Mineral. Soc. Am.*, vol. 8, pp. 128–134, 1923.

[27] E. Miklosy, J. Papp, and D. Kall, "Xylene isomerization on H-mordenites and H-clinoptilolites," *zeolites*, vol. 3, pp. 139–148, 1983.

[28] H. Sakoh, M. Nitta, and K. Amura, "Catalytic activity and selectivity of modified clinoptilolites for conversion of methanol to light olefines," *Appl. Catal.*, vol. 16, pp. 249–253, 1985.

[29] D. L. Bish and D. W. Ming, "Natural Zeolites: Occurrence, Properties, Application," *Rev. Miner. Geochemistry*, vol. 45, 2001.

[30] C. Baerlocher and L. B. McCusker, "Database of zeolite structure," *International zeolite association*, 2014. [Online]. Available: http://www.iza-structure.org/databases/.

[31] F. A. Mumpton, *Mineralogy and Geology of natural zeolites*, vol. 4. Mineralogical Society of America, 1981.

[32] J. Dong, Y. S. Lin, M. Kanezashi, and Z. Tang, "Microporous inorganic membranes for high temperature hydrogen purification," *J. Appl. Phys.*, vol. 104, no. 12, pp. 121301–1_121301–17, 2008.

[33] P. Swenson, B. Tanchuk, E. Bastida, W. An, and S. M. Kuznicki, "Water desalination and de-oiling with natural zeolite membranes — Potential application for purification of SAGD process water," *Desalination*, vol. 286, pp. 442–446, Feb. 2012.

[34] P. Swenson, B. Tanchuk, A. Gupta, W. An, and S. M. Kuznicki, "Pervaporative desalination of water using natural zeolite membranes," *Desalination*, vol. 285, pp. 68–72, Jan. 2012.

[35] H. Ashjian, Q. N. Le, D. N. Lissy, D. O. Marler, J. Shim, and S. S. F. Wong, "Naphthalene alkylation process," WO1991015443 A1, 1991.

[36] F. David, V. Vokhminz, and G. Ionova, “WATER CHARACTERISTICS DEPEND ON THE IONIC ENVIRONMENT. THERMODYNAMICS AND MODELISATION OF THE AQUO IONS,” *J. Mol. Liq.*, vol. 90, pp. 45–62, 2001.

[37] A. G. Volkov, S. Paula, and D. W. Deamer, “Two mechanisms of permeation of small neutral molecules and hydrated ions across phospholipid bilayers,” vol. 42, no. January 1996, pp. 153–160, 1997.

[38] J. Zhou, X. Lu, Y. Wang, and J. Shi, “Molecular dynamics study on ionic hydration,” *Fluid Phase Equilib.*, vol. 194–197, pp. 257–270, Mar. 2002.

[39] M. Y. Kiriukhin and K. D. Collins, “Dynamic hydration numbers for biologically important ions,” *Biophys. Chem.*, vol. 99, no. 2, pp. 155–168, Oct. 2002.

[40] S. Ueda, H. Munarn, and M. Koizumi, “Crystallization of mordenite from aqueous solutions,” vol. 65, no. l, pp. 1012–1019, 1980.

[41] D. Iglesia and P. Gorgojo, “Preparation and Characterization of Zeolite Membranes,” vol. 13, no. 07, pp. 135–175, 2008.

[42] K. W. Boddeker, “Commentary : Tracing membrane science,” *J. Memb. Sci.*, vol. 100, pp. 65–68, 1995.

[43] V. K. Gupta and I. Ali, “Chapter 5.Water Treatment by Membrane Filtration Techniques,” in *Environmental Water-Advances in Treatment, Remediation and Recycling*, Elsevier B.V., 2013, pp. 135–154.

[44] T. Matsuura, *Synthetic Membranes and Membrane Separation Processes*. CRC press, Inc, 1994.

[45] Y. S. Lin, I. Kumakiri, B. N. Nair, and H. Alsyouri, “Microporous Inorganic Membranes,” *Sep. Purif. Rev.*, vol. 31, no. 2, pp. 229–379, Jan. 2002.

[46] SIEMENS, “Comparison of Ceramic and Polymeric Membranes in Wastewater Treatment For the Oil and Gas, Rubber Processing and Palm Oil Industries,” 2011.

[47] M. . Mottern, J. . Shi, K. Shqau, D. Yu, and H. Verweij, “Chapter 34-Microstructural Optimization of Thin Supported Inorganic Membranes for Gas and Water Purificatio,” in *Advanced Membrane Technology and Applications*, N. N. Li, A. G. Fane, W. S. Winston Ho, and T. Matsuura, Eds. A JOHN WILEY & SONS, INC., 2008, pp. 899–994.

[48] S. Luque, D. Gomez, and J. R.Alvarez, “Industrial Applications of Porous Ceramic Membranes (Pressure-Driven Processes),” *Membr. Sci. Technol.*, vol. 13, no. 07, pp. 177–216, 2008.

[49] M. Çakmakce, N. Kayaalp, and I. Koyuncu, “Desalination of produced water from oil production fields by membrane processes,” *Desalination*, vol. 222, no. 1–3, pp. 176–186, Mar. 2008.

[50] Focus on Catalysts, “p-Xylene production costs reduced by new zeolite membrane,” 2003.

[51] A. Julbe, “Chapter 6. ZEOLITE MEMBRANES - SYNTHESIS , CHARACTERIZATION AND APPLICATION,” 2007.

[52] R. Sch, J. Caro, M. Noack, and P. K, “Zeolite membranes _ state of their development and perspective,” vol. 38, 2000.

[53] M. Kondo, M. Komori, H. Kita, and K.-I. Okamoto, “Tubular-Type Pervaporation Module With Zeolite NaA Membrane,” *J. Membr. Sci.*, vol. 133, pp. 133–141, 1997.

[54] Carreon, M. A., S. Li, J. L. Falconer, and R. D. Noble, “‘Alumina-Supported SAPO-34 Membranes for CO2/CH4 Separation,’” *J. Am. Chem. Soc.*, vol. 130, pp. 5412–5413, 2008.

[55] J. Romero, C. Gijiu, J. Sanchez, and G. M. R. A, “unified approach of gas, liquid and supercritical solvent transport through microporous membranes.,” *Chem. Eng. Sci.*

[56] S. D. Seader and E. J. Henley, *Separation Process Principles*. John Wiley & Sons, 2006.

[57] D. M. Ruthven, “Diffusion through Porous Media : Ultrafiltration , Membrane Permeation and Molecular Sieving,” vol. 11, no. 2009, pp. 1–2.

[58] T. C. Bowen, R. D. Noble, and J. L. Falconer, “Fundamentals and applications of pervaporation through zeolite membranes,” *J. Memb. Sci.*, vol. 245, no. 1–2, pp. 1–33, Dec. 2004.

[59] S. P. Nunes, K. V. Peinemann, Wiley-VCH, and Weinhim, “Membrane Technology in the Chemical Industry,” *J. Memb. Sci.*, vol. 59, no. 1, pp. 194–299, Jul. 2001.

[60] CRC for Greenhouse Gas Technologies, “http://www.co2crc.com.au/aboutccs/cap_membranes.html,” 2011. .

[61] H. WS and S. KK, *Membrane Handbook*. New York: Chapman and Hall, 1992.

[62] A. G. Fane, C. Y. Tang, and R. Wang, "4 . 11 Membrane Technology for Water : Microfiltration , Ultrafiltration , Nanofiltration , and Reverse Osmosis," 2011.

[63] C. Dotremont, S. Van den Ende, H. Vandommele, and C. Vandecasteele, "Concentration polarization and other boundary layer effects in the pervaporation of chlorinated hydrocarbons," *Desalination*, vol. 95, no. 1, pp. 91–113, Mar. 1994.

[64] C. H. Tan and H. Y. Ng, "Modified models to predict flux behavior in forward osmosis in consideration of external and internal concentration polarizations," *J. Memb. Sci.*, vol. 324, no. 1–2, pp. 209–219, Oct. 2008.

[65] G. Schock and A. Miquel, "Mass transfer and pressure loss in spiral wound modules," *Desalination*, vol. 64, pp. 339–352, 1987.

[66] T. D. Waite, A. I. Schaefer, and A. G. Fane, *Nanofiltration:Principles and applications*, 1st ed. New York, N.Y.: Elsevier, 2005.

[67] H. Suzuki, "Composite membrane having a surface layer of an ultrathin film of cage-shaped zeolite and processes for production thereof," 4,699,892, 1987.

[68] The 1st FEZA school on zeolites, Prague, Czech Republic, "Zeolites and ordered mesoporous materials: progress and prospects," in *Studies in surface science and catalysis*, J. Cejka and H. va. Bekkum, Eds. Elsevier, 2005.

[69] D. L. Wernick and E. J. Osterhuber, "Permeation through a single crystal of zeolite NaX," *J. Memb. Sci.*, vol. 22, pp. 137–146, 1985.

[70] P. Kolsch, D. Venzke, M. Noack, P. Toussaint, and J. Car, "Zeolite-in-metal Membranes: Preparation and Testing," vol. 2, pp. 2–3, 1994.

[71] Z. Lin, "Synthesis and characterisation of titanosilicate ETS-10 membranes," *Microporous Mesoporous Mater.*, vol. 67, no. 1, pp. 79–86, Jan. 2004.

[72] G. Clough, "Review of CSD-13 Water and Sanitation Decisions in: STATEMENT OF THE UNITED NATIONS INDUSTRIAL DEVELOPMENT ORGANIZATION At THE COMMISSION ON SUSTAINABLE DEVELOPMENT," New York, 2008.

[73] C. V. Deutsch and J. A. Mclennan, *Guide to SAGD (Steam Assisted Gravity Drainage) Reservoir Characterization Using Geostatistics*, vol. 3. 3-133 Markin/CNRL Natural Resources Engineering Facility, Edmonton, AB, Canada T6G 2W2: Centre for Computational Geostatistics., 2005.

[74] B. R., "The potential for horizontal wells for petroleum production.," *J Can Pet Technol.*, vol. 28, pp. 39–47, 1989.

[75] W. F. Heins and GE Water Technologies Process, "Technical Advancements in SAGD Evaporative Produced Water Treatment," *JCPT*, vol. 48, no. 11, pp. 27–32, 2009.

[76] *Dow Water & Process Solutions FILMTEC ™ Reverse Osmosis Membranes Technical Manual*. The Dow Chemical Company (1995-2013).

[77] W. H. Goodman, M. R. Godfrey, T. M. Miller, Nalco company, Naperville, and IL, "Scale and Deposit Formation in Steam Assisted Gravity Drainage (SAGD) Facilities," in *The InternationalWater Conference*, 2010, pp. 24–28.

[78] W. Heins and D. Peterson, "Use of evaporation for heavy oil produced water treatment.," *J Can Pet Technol.*, vol. 44, pp. 26–30, 2005.

[79] St. Cloud Mining Company, "St . Cloud Natural Zeolite (Clinoptilolite)," New Mexico, 2007.

[80] Graver Technologies, "Proven technology for the most challenging separations," 2007.

[81] D. Chen, L. He, and S. Shang, "Study on aluminum phosphate binder and related Al2O3-SiC ceramic coating," *Mater. Sci. Eng.*, vol. 348, pp. 29–35, 2003.

[82] A. S. Wagh, *Chemically Bonded Phosphate Ceramics*. Elsevier, 2004, pp. 121–133.

[83] Accumet Materials Co., "http://www.accumetmaterials.com." [Online]. Available: http://www.accumetmaterials.com/new/refractobond.htm.

[84] EPCOR, "Water Quality 2013, 2.1.2 Summary of major chemicals, microbiological, and physical parameters of Edmonton drinking water," edmonton, 2013.

[85] K. Jittavanich, C. B. Clemons, K. L. Kreider, M. Aljarrah, E. Evans, and G. W. Young, "Modeling, simulation and fabrication of coated structures

using the dip coating technique," *Chem. Eng. Sci.*, vol. 65, no. 23, pp. 6169–6180, Dec. 2010.

[86] M. Hayes and S. B. G. O'Brien, "A model for gravity driven flow of a thin liquid-solid solution with evaporation effects," *Zeitschrift für Angew. Math. und Phys.*, vol. 56, no. 5, pp. 852–873, Sep. 2005.

[87] P. Yimsiri and M. R. Mackley, "Spin and dip coating of light-emitting polymer solutions: Matching experiment with modelling," *Chem. Eng. Sci.*, vol. 61, no. 11, pp. 3496–3505, Jun. 2006.

[88] O. F. Evaporation, O. N. Thin, F. Deposition, and I. N. D. I. P. Coating, "rights reserved 0735.1933/02/$-see front matter," vol. 29, no. I, pp. 35–44, 2002.

[89] C. H. Lee, Y. Lu, and A. Q. Shen, "Evaporation induced self assembly and rheology change during sol-gel coating," *Phys. Fluids*, vol. 18, no. 5, p. 052105, 2006.

[90] Y. Takahashi, S. Okada, R. Bel Hadj Tahar, K. Nakano, T. Ban, and Y. Ohya, "Dip-coating of ITO films," *J. Non. Cryst. Solids*, vol. 218, pp. 129–134, Sep. 1997.

[91] D. L. Bish, "Effects of Exchangeable Cation Composition on the Thermal Expansion/Contraction of Clinoptilolite," *Clays Clay Miner.*, vol. 32, no. 6, pp. 444–452, 1984.